THE UNIVERSITY OF MICHIGAN

INDUSTRY PROGRAM OF THE COLLEGE OF ENGINEERING

HYDRATION OF N-BUTENE WITH CATION EXCHANGE RESIN

William James Murray Douglas

A dissertation submitted in partial fulfillment
of the requirements for the degree of
Doctor of Philosophy in the
University of Michigan
1958

March, 1959

IP-357

ersn

UMR0969

Doctoral Committee:

Professor Robert R. White, Chairman
Professor Julius T. Banchero
Associate Professor Ben Dushnik
Doctor Jacob Eichhorn, Dow Chemical Co.
Associate Professor Robert W. Parry

ACKNOWLEDGEMENTS

The writer wishes to express his thanks to the members of the doctoral committee for their participation in this research. In particular, sincere appreciation is extended to the committee chairman, Professor Robert R. White, whose counsel throughout the course of the investigation contributed in many ways to the completion of the work. A number of graduate students helped through discussions of problems. Lowell Yemin assisted in the early runs, and continued to be a ready source of aid and advice. Richard C. Faulkner rapidly became an expert on the installation of reactor liners. A special thanks is due M.T. Tayyabkhan, who unstintingly shared in the working-out of many aspects of the research.

Financial assistance in the form of fellowships from the Visking Corporation and The Dow Chemical Company are also gratefully acknowledged.

Finally, the writer wishes to thank his family; his wife for her patience and assistance, and Donald, whose candor was never lost under the pressure of events.

SUMMARY OF RESULTS

The hydration of liquid n-butene to sec-butyl alcohol using a cation exchange resin catalyst was studied in a flow reactor under steady-state conditions. The experimental variables investigated were:

Temperature 115° to 145°C
Resin size 50 - 400 mesh
Resin weight 5 - 60 gms.
Resin crosslinkage 8% and 12% divinylbenzene
Superficial liquid velocity 40 - 1100 cm/hr.
Butene conversion (hydration) 12.2% max.
Alcohol conversion (dehydration) 30.7% max.
Feed composition
Mol % butene 20 - 82%
Mol % alcohol 0 - 25%

Integral reaction rates were measured as a function of temperature and space velocity. The initial chemical reaction rate for the two liquid phase feed was correlated by the equation

$$r_i = 9.0 \times 10^{10} \exp(-24800/RT) \frac{\text{g mols}}{(\text{hr})(\text{gm HR})}$$

which indicates an activation energy of 24800 cal/mol for the 8% crosslinked, sulfonated polystyrene resin catalyst used.

The following values were determined for the volumetric efficiency of the resin:

Resin mesh size	Volumetric Efficiency, ϕ
50 - 100	89%
100 - 200	97%

These values indicate that resin phase diffusion is not a major determinant of reaction rate for this system.

For resin of 100 - 200 mesh size, the reaction rate did not become independent of liquid flow rate until the superficial liquid velocity was increased to about 1100 cm/hr. The existence of a large mass transfer resistance within the liquid phases at lower velocities may be ascribed to the presence of two almost completely immiscible liquid phases.

Equilibrium conversions of n-butene of from 8 to 12% were measured for the liquid phase reaction and were correlated with temperature and butene content of the feed. Equilibrium conditions were approached from both hydration and dehydration. The slopes of several liquid-liquid tie-lines representing simultaneous chemical and phase equilibrium were determined from equilibrium conversions obtained with feeds of two different butene/water ratios. These measurements confirmed the prediction that the alcohol content of the butene-rich phase is much greater than that of the corresponding water-rich phase.

Estimates of the desulfonation rate of the resin in the environment of the butene hydration reaction indicate that it would take 2 1/2 years at 145°C for the resin to be 50% desulfonated.

Exploratory experiments indicate that both the resin catalyzed reaction rates and the position of chemical equilibrium are more favorable for the hydration of propylene than for butene.

It was found that the cation exchange resin could replace sulfuric acid in the two-step esterification-hydrolysis process for making sec-butyl alcohol. In this sense, therefore, the cation resin may be said to act chemically as a strong acid. Within the limitations of the data obtained, the hydration rates by the two step process appeared to be much lower than for the continuous catalytic process.

TABLE OF CONTENTS

LIST OF TABLES

LIST OF ILLUSTRATIONS

I INTRODUCTION

The catalytic properties of various ion exchange materials have been known for many years. It is only within the last decade, however, that the use of synthetic organic ion exchange resins as catalysts has been investigated. Those cation exchange resins which act as strong, highly ionized acids have been found to catalyze many reactions which are catalyzed by strong inorganic liquid acids such as sulfuric or hydrochloric acids. (9)(17)(19)

Some of the advantages of the solid resin acid catalysts are listed below:

(1) No acid separation or neutralization step is required since the resin is a solid.

(2) Continuous processes are conveniently designed by passing the reactants over fixed beds of resin.

(3) Some undesirable side reactions encountered with strong inorganic acids may be avoided.

(4) The catalyst has a potentially long life, thus reducing catalyst costs.

(5) Unusual selectivity effects not found with liquid acids may be found in some cases, and are believed to be associated with the reduced degrees of freedom of the solid acids. (13)

(6) Equipment costs may be reduced since the handling of corrosive inorganic acids is avoided.

Although a considerable number of reactions have been investigated with ion exchange resins as catalysts, most of these were chosen for convenience in demonstrating and defining the technique, or were for the synthesis of chemicals not of significant industrial importance. The hydration of normal butene to secondary butyl alcohol was chosen for this study after preliminary experiments indicated that the reaction rate with a cation exchange resin catalyst was in the commercially attractive range. Also, this reaction, as well as being itself of current commercial importance, represents one of the series of industrially important hydrations of mono-olefins to secondary alcohols. In the case of secondary butyl alcohol, the production rate amounts to about 38 million gallons annually. Its principal uses are for the production of methyl ethyl ketone, secondary butyl acetate, lacquers, and miscellaneous solvents.

Up to the present, two basically different types of processes for this hydration reaction have been developed. In the continuous catalytic vapor phase process, butene and water at high temperatures and pressures are passed over a solid-supported, inorganic acid-type catalyst. The other, and more industrially popular process, involves a two-step synthesis, using sulfuric acid to absorb and esterify the butene in the first step, and hydrolysis of the mono-butyl sulfate to the secondary alcohol in the second step. In the present study the major focus will be a continuous liquid phase process using a cation exchange resin as the catalyst.

In the 1958 edition of his book "Ion Exchange Resins," Kunin (16) states, "Except for these few industrial examples, the use of ion exchange resins as catalysts still remains a laboratory curiosity." It is believed that the present study removes this fascinating tool one step further from the status of a curiosity.

II THEORETICAL ORIENTATION OF THE STUDY

The experimental approach of the study was determined by the nature of the various equilibria and rate processes involved. Phase equilibria between the two liquid phases present, and between liquid and resin, as well as the chemical equilibrium of the hydration reaction, define the limiting conditions. Mass transfer rates within the liquid phases, and diffusional and chemical reaction rates within the resin determine the rate of approach to the limiting conditions. It will be seen that the peculiarities of this particular reaction system make inapplicable a number of techniques and approaches which have been used in similar studies.

Phase Equilibrium Relations of the Liquid Reactants

The data of Alexejew and others (14), (see page 5 Figure 1), show that sec-butyl alcohol and water are only partially miscible at low temperatures. The extent of the two phase region decreases as the temperature is increased until the components become completely miscible at the critical solution temperature of 113.1°C. Liquid butene and water are almost completely immiscible at all temperatures, whereas sec-butyl alcohol and butene are completely miscible liquids. Since the ternary phase diagram for sec-butyl alcohol, water and butene may be viewed as an extension of the three binary phase diagrams into the corresponding three-component system, it is

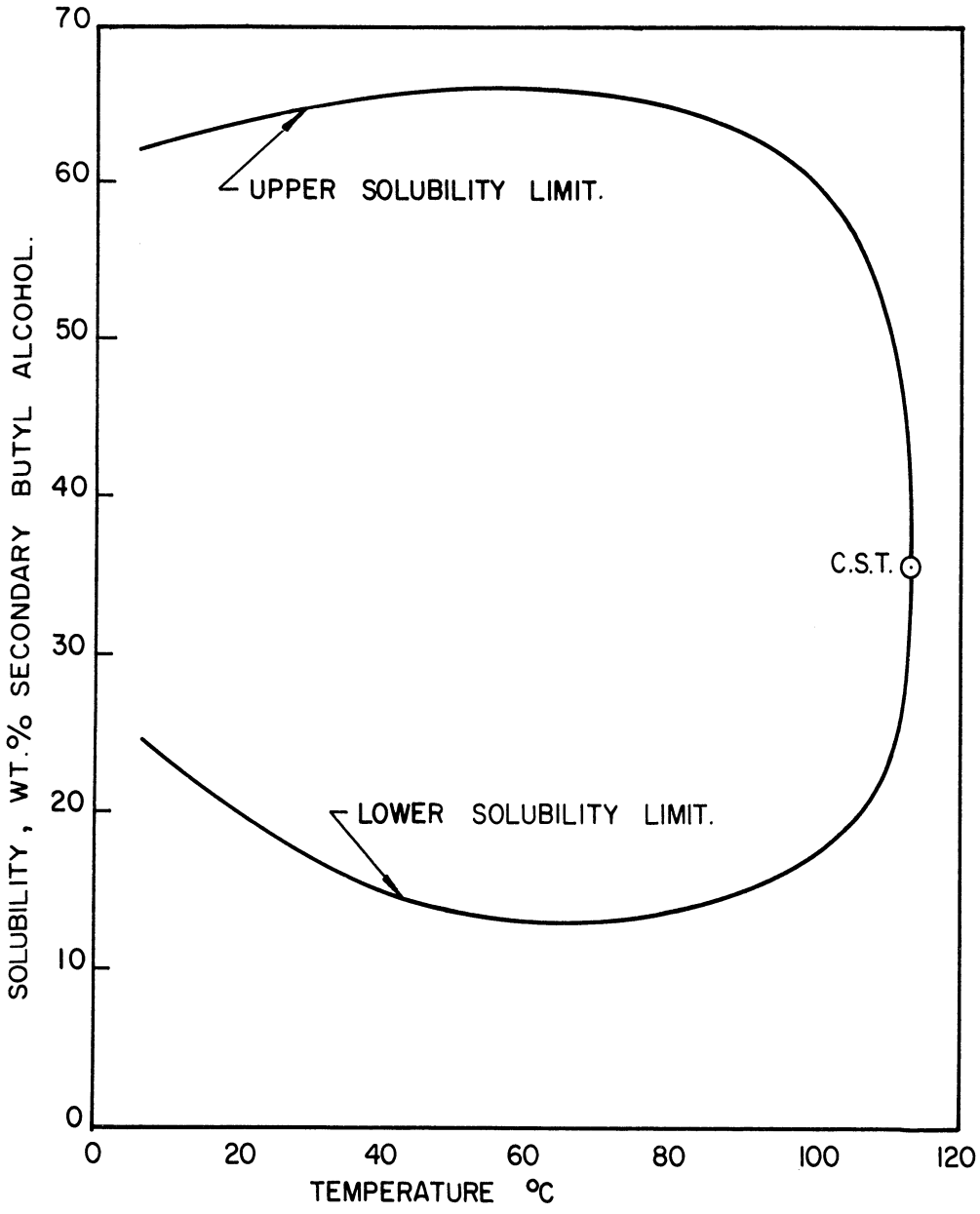

Figure 1. Liquid-Liquid Solubility Curve for Secondary Butyl Alcohol-Water.

seen that the latter will contain a large region of two liquid phases in equilibrium. (c.f. Figure 2) For the ternary system, neither the liquid-liquid solubility curve nor the equilibrium tie-lines at any temperature have been reported.

Because of the pressure, about 550 psia, required to maintain the system in a completely liquid state at the highest temperature involved in this study, an accurate determination of this liquid-liquid phase equilibrium information would, in itself, be a major undertaking. However, as a guide to planning the study, the phase behavior of this system may be approximated from an examination of the data for many similar hydrocarbon-alcohol-water systems as collected by Seidell (22). For example, this author includes liquid phase equilibrium data for the system propylene-isopropyl-alcohol-water. With these guides, the liquid-liquid solubility curve in the pertinent range of temperatures has been approximated as shown on Figure 2. Variation in the slope of tie-lines connecting the composition points of two phases in equilibrium in the ternary system may also be deduced in the absence of direct experimental data. At any temperature below the sec-butyl-alcohol-water critical solution temperature of 113.1°C, the liquid-liquid solubility isotherms for the ternary enclose an area which extends from the butene-water base to the alcohol-water side of the phase diagram. It follows that the slope of the tie-lines changes rapidly from being parallel to the butene-water base to running parallel to the alcohol-water side. Since the temperature range of the present investigation

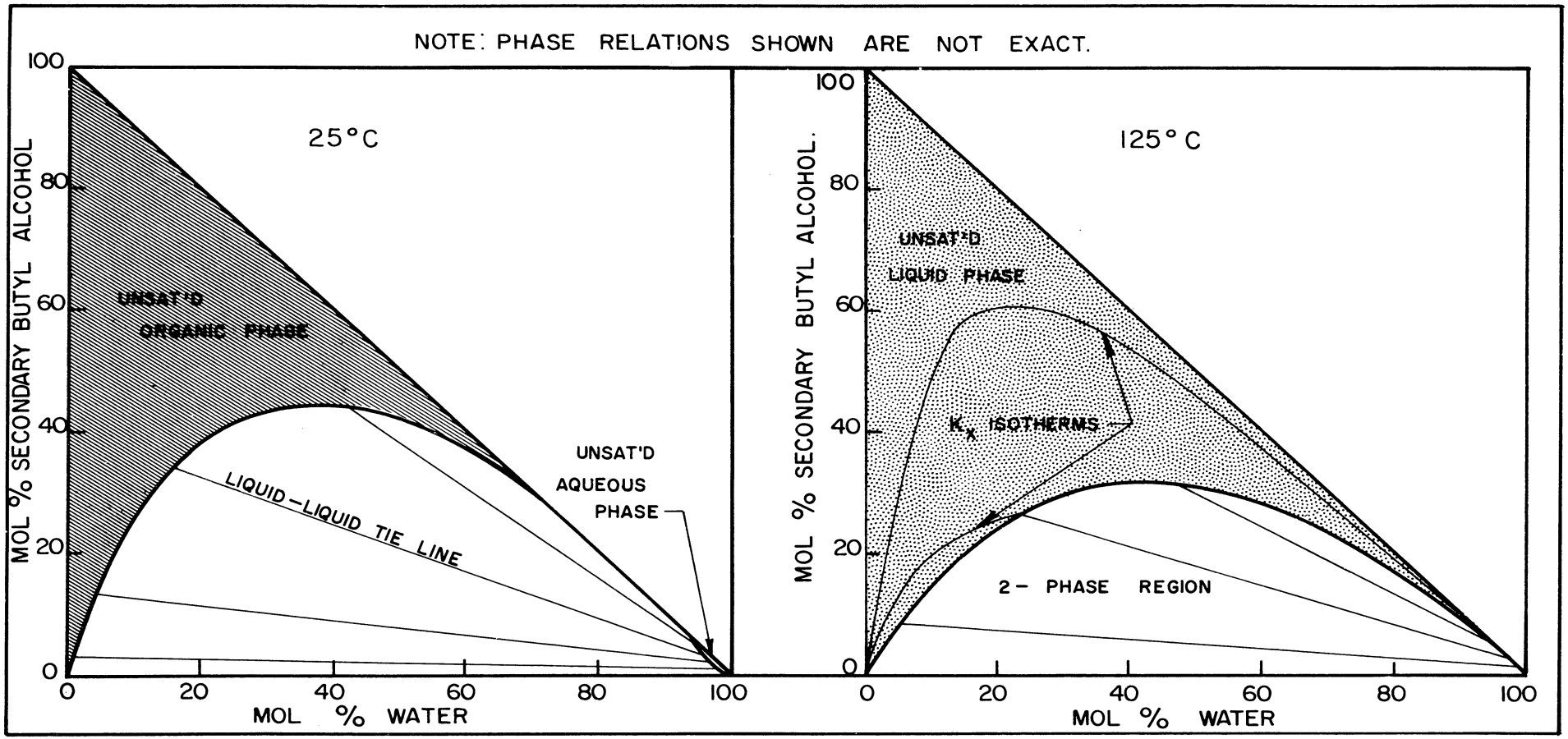

Figure 2. Ternary Liquid Phase Diagrams.

begins just above the critical solution temperature, it follows that the alcohol content of the butene rich phase will be in general much greater than that of the corresponding equilibrium aqueous phase.

Chemical Equilibrium for the Liquid Reactants

The chemical equilibrium for the hydration of n-butene to sec-butyl alcohol has been studied by a number of investigators (18)(26). These studies show that the position of equilibrium becomes more favorable as the temperature is decreased, which is consistent with the exothermic nature of the hydration reaction. These data were all obtained from vapor phase operations, conducted at high temperatures and in part also at high pressures. Their use for the present relatively low temperature, liquid phase study therefore presents considerable difficulty. The experimental data of these investigators can be most usefully expressed in terms of equilibrium constants based on thermodynamic activities, which can be calculated with reasonable accuracy from their experimental vapor phase compositions. While these reaction equilibrium constants may be extrapolated with some confidence to the temperature range of this study, the calculation of equilibrium liquid phase compositions from these equilibrium constants requires the corresponding liquid phase activity coefficients. The highly non-ideal nature of the liquid ternary however, precludes obtaining these activity coefficients by any method other than direct experimental measurement. Again,

as was the case for the phase equilibrium study discussed earlier, the determination of these activity coefficients would require a comprehensive investigation at pressures up to 550 psia. Since the use of the existing equilibrium constants would necessitate this additional study, the alternative of direct measurement of the chemical equilibrium relations for the liquid-phase reaction was considered. By using different operating conditions, the same flow reactor used for the reaction rate experiments may be used to determine the chemical equilibrium relations. Equilibrium concentrations can be approached from both sides, that is, from dehydration as well as from hydration, in order to improve the reliability of the equilibrium values obtained. The method of direct measurement of chemical equilibrium was chosen since it was believed that more accurate results would be obtained.

Butene Hydration Reaction Rate Studies

Chemical reaction rates for the hydration of normal butene have been measured by a number of authors. Detailed rate studies of the high temperature (150° - 400°C), high pressure (to 10,000 psi) vapor phase hydration have been carried out by several workers, including Marek and Flege (18), and Dale, Sleipcevich and White (8). Also, the extensive patent literature on this process contains an additional body of more

fragmentary reaction rate data. Besides the vapor phase studies, a number of investigations have been made of the two-step hydration process. In this process the butene is first esterified with an inorganic acid such as sulfuric acid to form the mono-butyl sulfate, which, in the second step of the process, is hydrolyzed to secondary butyl alcohol (c.f. summaries by Ellis (10) and Goldstein (11).) The focus of the current study, that is, continuous catalytic hydration in the liquid phase using a porous solid acidic catalyst, does not overlap the above investigations, and provides reaction rate information on a type of operation not previously studied.

Ion Exchange Resin Catalyst

The composition and properties of the cation exchange resin used has a controlling effect on the reaction. These resins may be divided into two main types, the weak acid resins containing carboxylic or phenolic groups, and the strong acid resins containing sulfonic or phosphonic groups. Since for reactions catalyzed by acids the reaction rate is usually proportional to the activity of the hydrogen ions, the weak acid resins are not generally attractive as catalysts. Among the strong acid resins, the most thoroughly developed and generally attractive type is sulfonated polystyrene, cross-linked with divinylbenzene. The amount of divinylbenzene used is limited by the properties desired for the final sulfonated product.

For less than 4% divinylbenzene the resin beads begin to swell excessively in aqueous liquids, and the relatively high solubility of the resin makes them commercially unattractive. On the other hand, resins crosslinked with more than 12% divinylbenzene tend to form very rigid, non-swelling beads, in which the diffusional resistance for most materials becomes unpractically high. For most systems the optimum crosslinkage corresponds to about 8% divinylbenzene. It is this resin which was chosen for the present study. The structure of this three-dimensional polymer is illustrated schematically below:

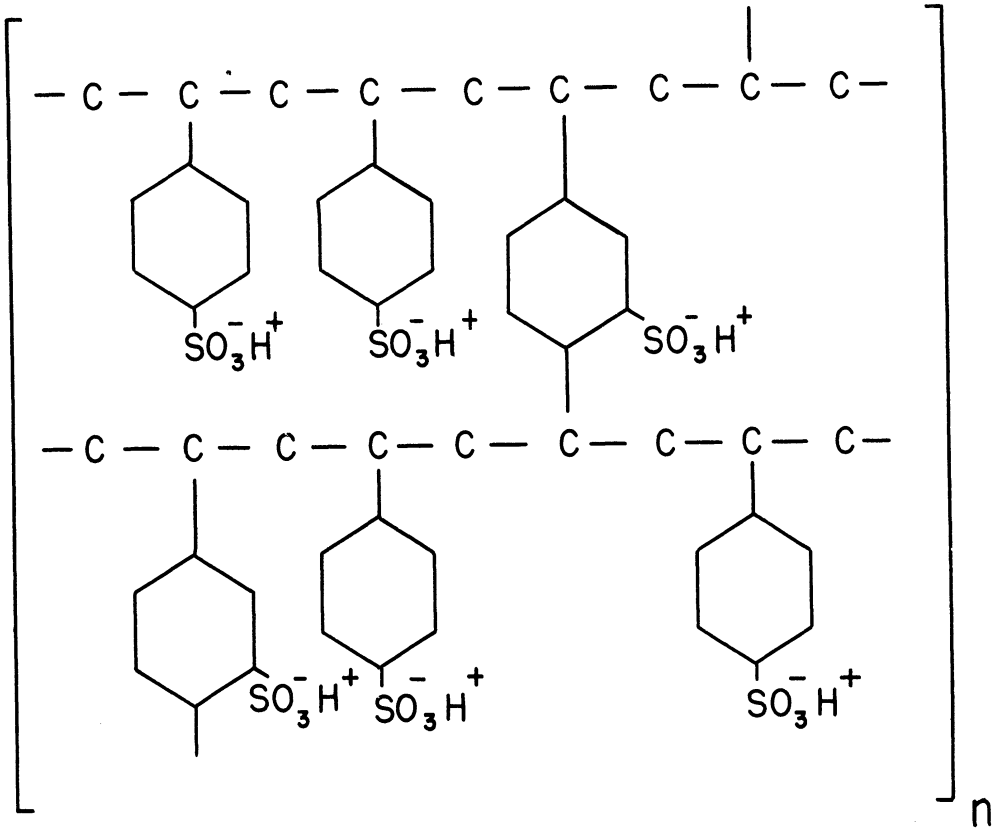

Since the polystyrene network is sulfonated by reaction with concentrated sulfuric acid, the reverse process, that is, hydrolysis of the sulfonated resin, must also be considered.

This reversible reaction may be represented as:

$$\left[\emptyset - H\right]_n + n\ H_2SO_4 = \left[\emptyset - SO_3^-H^+\right]_n + n\ H_2O$$

in which $\emptyset$ represents the organic monomer base of the resin. For any reaction in the presence of water, the rate of hydrolysis of the resin may be taken as the rate of deactivation of the catalyst, provided that

(1) the resin does not depolymerize at the reaction temperature,

(2) there are no cations in the system to exchange with the hydrogen ions of the resin, and

(3) that the resin does not become fouled with reaction products or by-products.

Boyd, et al (5) investigated the stability of sulfonated polystyrene resins in the hydrogen form by heating them with water in a quartz tube. They found that hydrolysis of the resin occurred before the resin began to depolymerize, and that above 180°C the desulfonation rate became quite rapid. Bauman, et al (4) also give fragmentary hydrolysis rates at high temperatures. It is evident that the existing data are not sufficient to estimate resin life for the conditions of the system under study. Also, since the hydrolysis rate increases

with temperature, the resin desulfonation will impose an upper temperature limit on the practical range of use of a particular resin.

The effectiveness of cation exchange resins as catalysts has now been investigated for a considerable number of reactions. These are summarized regularly by Kunin,et al (2) and others (1). Some of the types of reactions which are known to be catalyzed by cation resins are esterifications, ether and acetal formations, alcoholysis reactions, hydrolyses, dehydrations, cumene hydroperoxide decomposition, and aldol condensations. Some of these investigations have been only semi-quantitative, only a few have concerned reactions of current industrial significance, and little attention has been given the question of resin life. Also, most of the above reactions were known to react rapidly in the presence of conventional acid type catalysts, whereas butene hydration rates are relatively slow. Because of the slow hydration rates, the use of operating temperatures higher than in any of the above studies was anticipated. This study provides, therefore, an appreciable extension of knowledge of the catalytic effectiveness of sulfonated crosslinked polystyrene resins.

Theoretical Analysis of Heterogeneous Reaction System

The reaction system consists of a bed of resin spheres and a feed of constant inlet composition flowing at a steady rate through the bed, which is maintained at a constant tem-

perature. Once steady state has been established, compositions at all points in the bed are invariant with respect to time. At steady state four basic factors can be distinguished which together determine the overall hydration rate. These are:

(1) mass transfer rates of reactants from the liquid to the resin surface and of the product in the opposite direction,

(2) the phase equilibrium relation between resin phase concentrations at the resin surface and concentrations in the immediately adjoining liquid stream,

(3) the diffusion rate of reactants from the surface of the resin spheres into the resin, and the corresponding outward diffusion of the reaction product, and

(4) the rate of reaction within the resin phase.

If the liquid flow rate is sufficiently high, the mass transfer resistance can be neglected, and the rate of disappearance of a reactant becomes dependent upon its reaction rate and its diffusion rate within the resin sphere. Mathematical techniques have been developed by Smith and Amundsen (25) and by Saletan and White (21) for handling the problem of simultaneous diffusion and chemical reaction in beds of spherical resin particles. Since the more generally applicable method of Saletan will in part be used in this study, a description of this approach will be given.

By definition of the steady state condition, the net rate of diffusion of a reactant into any spherical lamina of a resin bead must be equal to the rate at which it disappears by reaction in the lamina. A non-linear second order differential equation in reactant concentration and resin radius may be obtained by using Fick's law to relate the diffusion rates to concentration gradients, and a postulated reaction mechanism to relate reaction rates to concentrations. A number of approximations reduces this differential equation to a Bessel's equation of one-half order, the solution of which follows directly. The solution obtained expresses the radial concentration gradients of any of the reactants as a function of radius and concentration at the resin surface. From the concentration gradient at the resin surface, an expression may be obtained for the volumetric average rate of reaction within the resin bead. From this expression one can separate a group of terms which represent the reaction rate at the resin surface. The remaining terms may therefore be considered as an efficiency factor, since they represent the ratio of the volumetric average reaction rate to the reaction rate at the surface of the resin bead. This efficiency factor, designated ϕ by Saletan, is an analytic function of R, (the resin radius) and τ, (a collection of terms involving reaction rate constants and diffusivities of the components in the resin phase). The form of the efficiency factor is

$$\phi = \frac{3\tau}{R} \left(\coth \frac{R}{\tau} - \frac{\tau}{R} \right)$$

and is reproduced from Saletan as Figure 3 . Having thus obtained an expression relating volumetric average reaction rate to resin surface concentrations and the efficiency factor ϕ, there remains only the step of replacing resin surface concentrations with liquid phase concentrations. This is accomplished by use of equilibrium phase distribution coefficients, α, representing the ratio of resin phase to liquid phase concentration for any component. Thus a differential equation is obtained relating reaction rate to liquid phase composition and to an efficiency factor representing the diffusional resistance within a resin bead. This differential equation may be integrated to yield integral conversion data for a flow reactor.

Application of the Efficiency Function Analysis to the Present Study

The setting up and solution of the Saletan analysis for ion exchange catalysis involves a number of assumptions and simplifications which are not applicable to the present system. The highly non-ideal nature of the ternary liquid reactants make it most unlikely that any reaction rate expression in terms of concentrations would be applicable beyond a very limited range of composition. A rate expression in terms of thermodynamic activities would require activity coefficients which would be sensitive functions of concentration due to the nature of the system phase behavior. The difficulty of measuring these activity coefficients has already been discussed. Similarly, for all systems analyzed by this method, c.f. Saletan

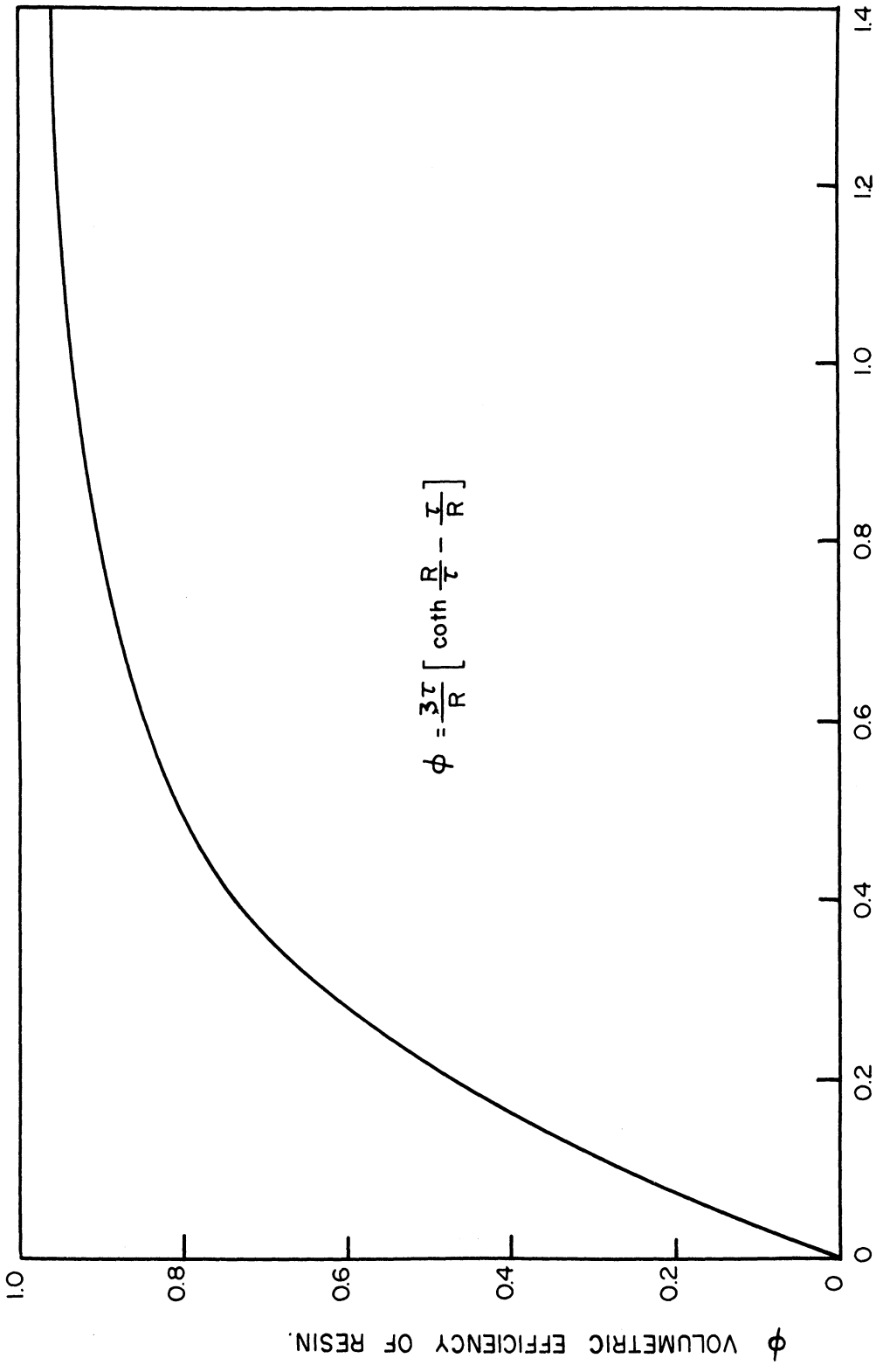

Figure 3. Resin Efficiency Function.

(21), Barker (3), and Klein (15), it has been possible to adequately represent chemical equilibrium by an equilibrium constant in terms of concentrations, and to represent liquid phase-resin phase distribution ratios and the resin phase diffusivities of each component as constants, independent of concentration. For the butene-water-butyl alcohol system the first two of these simplifications are wholly inadequate and the third is highly improbable. It must be concluded that the reaction system variables as a whole cannot be analyzed by this method, since even if all the missing thermodynamic data were available, the differential equations which result cannot be solved.

However, one aspect of the Saletan analysis, that is the variation of the efficiency function, ϕ , with resin radius, R, will remain the same in spite of the difficulties in applying the entire analysis. It should be noted that for the acetone condensation reaction, Klein (15) was unable to derive a satisfactory ϕ function from the theoretical basis derived by Saletan. In spite of this, he was able to use the theoretical form of the relation to empirically determine satisfactory values of ϕ as a function of resin size. In an analogous manner the theoretical form of the efficiency function resin radius relation will be used in this study to evaluate the approach to 100% resin efficiency obtained with small diameter resin beads.

Scope of the Present Study

Following the consideration of the equilibria and rates involved for this particular resin catalyzed system, and the difficulties in obtaining a comprehensive mathematical treatment, the following study was carried out. Integral reaction rates were measured over the interesting range of temperature at a number of space velocities, using relatively small resin beads so that the resin phase diffusional resistance was negligible (i.e. operating with resin efficiency factors approaching unity). These integral reaction rates were extrapolated to initial reaction rates, which in turn are correlated with temperature. Hydration rates were measured for binary and ternary liquid feeds, with the total feed composition falling both inside and outside the two phase liquid envelope. Four other factors that affect reaction rates, that is, liquid phase mass transfer resistance, the ratio of the two liquid phases, percent crosslinkage of the resin, and resin life were also studied. The position of chemical equilibrium as a function of temperature and feed composition was determined by approaching equilibrium from both sides in a flow reactor operated at low space velocities.

In addition to these studies of the continuous catalytic hydration of normal butene, two exploratory investions were made:

(1) The feasibility of operating the conventional two-step esterification-hydrolysis alcohol process with cation

exchange resin replacing the sulfuric acid.

(2) A few runs on hydration of propylene were made to evaluate roughly the applicability of the continuous resin catalyzed process to this homologous olefin.

III EXPERIMENTAL EQUIPMENT

Flow Diagram

The flow diagram is shown on Figure 4. Butene is stored in an insulated pressure vessel, one cubic foot in volume. The butene is kept as a liquid at room temperature by maintaining a pressure of about 40 psi from a helium cylinder through a water seal. The level of the water seal can be assurately read in a calibrated gaging cylinder, and these readings are used to determine the volumetric flow of butene to the reactor.

Water, (at times aqueous sec-butyl alcohol solution) is stored in the other gaging cylinder under the same pressure of helium as above. The gage level readings of this calibrated cylinder are used to accurately measure the water flow rate.

The reciprocating piston-type pump delivers each liquid separately to a pair of helium loaded surge vessels. The pulsations in liquid flow rate from the piston delivery of the pump can be almost eliminated by selection of an appropriate helium charge for the surge vessels.

The liquid feed streams enter the reactor from the opposite sides of an inlet tee. Two stainless steel cones, each containing a 0.006" diameter hole, were placed at the entrances to the inlet tee so that each liquid stream had to pass through

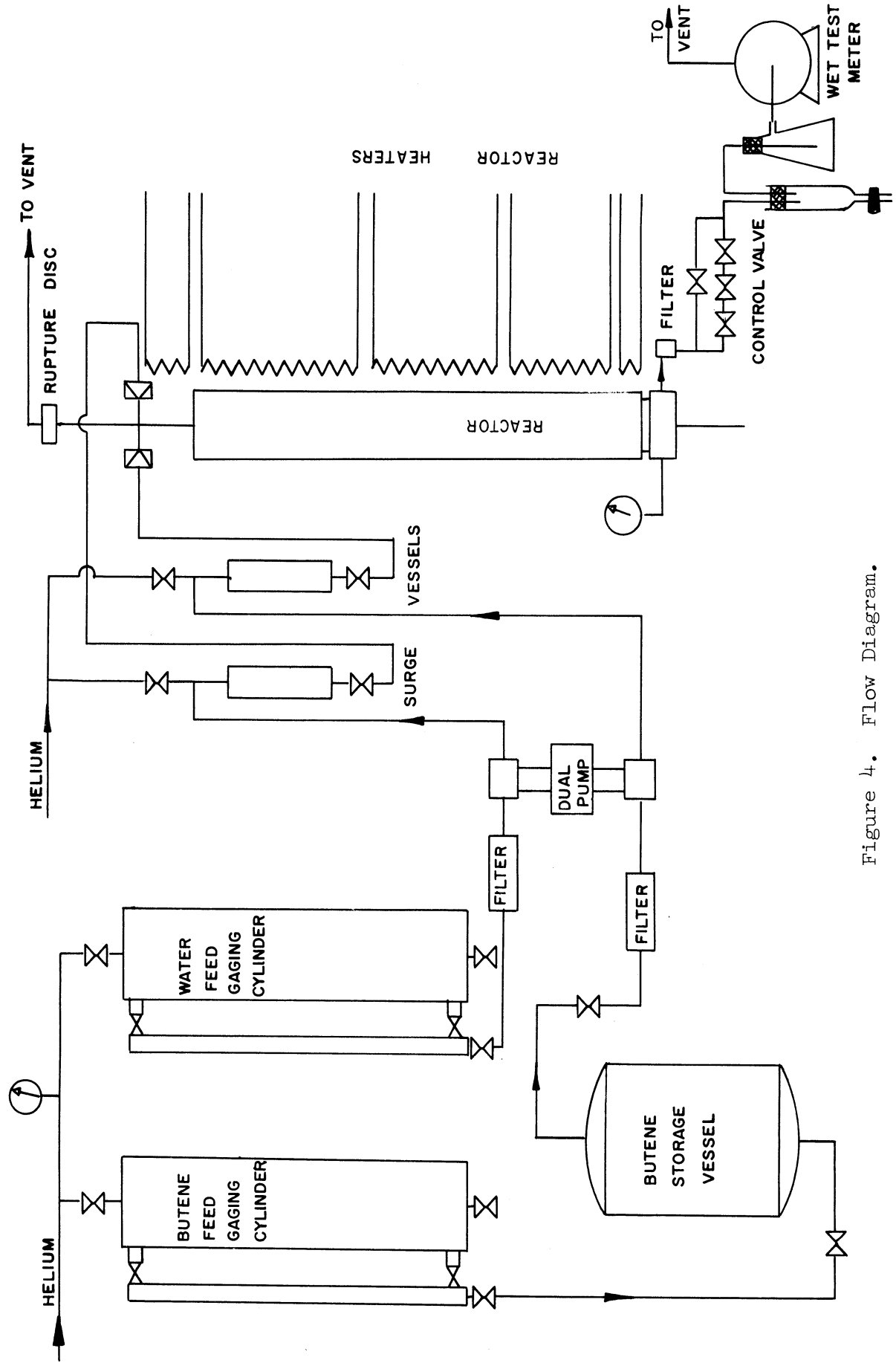

Figure 4. Flow Diagram.

this small orifice just before the streams mixed. This device was designed to break up the two immiscible liquid feed streams, although the break-up would probably not be sufficient to cause emulsification.

The liquid reactants pass downwards over the bed of resin catalyst, and leave the reactor at the bottom. A gas loaded back-pressure control valve maintains the reactor pressure at 600 psi and allows the product to flow out at a steady rate. Downstream of the pressure control valve the butene flashes at atmospheric pressure. The liquid and gas products are separated at the inlet of the liquid product receiver. The butene-rich gas phase is first passed through a water bubbler, then through a wet test meter, and finally is discharged to the atmosphere.

Much of the equipment used for this study was constructed earlier for an investigation of the dehydration of n-butyl alcohol (24). Details of this original equipment may be found in the dissertations of Sleipcevich (23) and Dale (7). However, a discussion of the equipment modifications required for the present hydration study are given below.

Pump

Sleipcevich and Dale used a Hills-McCanna pump, type HAJD-3/8", dual unit. It had, however, given undependable service. The source of the trouble was occasional severe back-leakage

through any of the four conical check-valves (one suction and one discharge check valve for each side of the dual pump). This difficulty continued to recur during the early part of the present investigation, but was solved by the replacement of the original male check valves with a set of four check valves of quite different design. The basic change in design was to lower considerably the center of gravity of the male conical element. In operation this piece alternately lifts to allow passage of fluid, then drops back into the mating conical seat in order to prevent any back-flow during the other half of the pumping cycle. Although considerable pressure is applied on top of the male check valve once it has seated, the initial positioning of the check valve is determined solely by gravity. It was therefore concluded that slightly imperfect mating of the conical surfaces was quite possible when the center of gravity of the moving piece was considerably above the mating area. The check valve assembly, including both male check valve designs, is shown on Figure 5. The original male check valves were manufactured from an extremely hard alloy, Hastelloy D. The new pieces were machined from a research alloy of equivalent hardness, provided by Dr. R. Decker of the University of Michigan. After careful machining the conical surface was polished with fine emory cloth.

To obtain completely dependable performance, it was also necessary to take a light cut of relatively soft stainless steel from the female conical seats. A new seat was then formed by one sharp tap on top of the assembled check valve. The seat thus

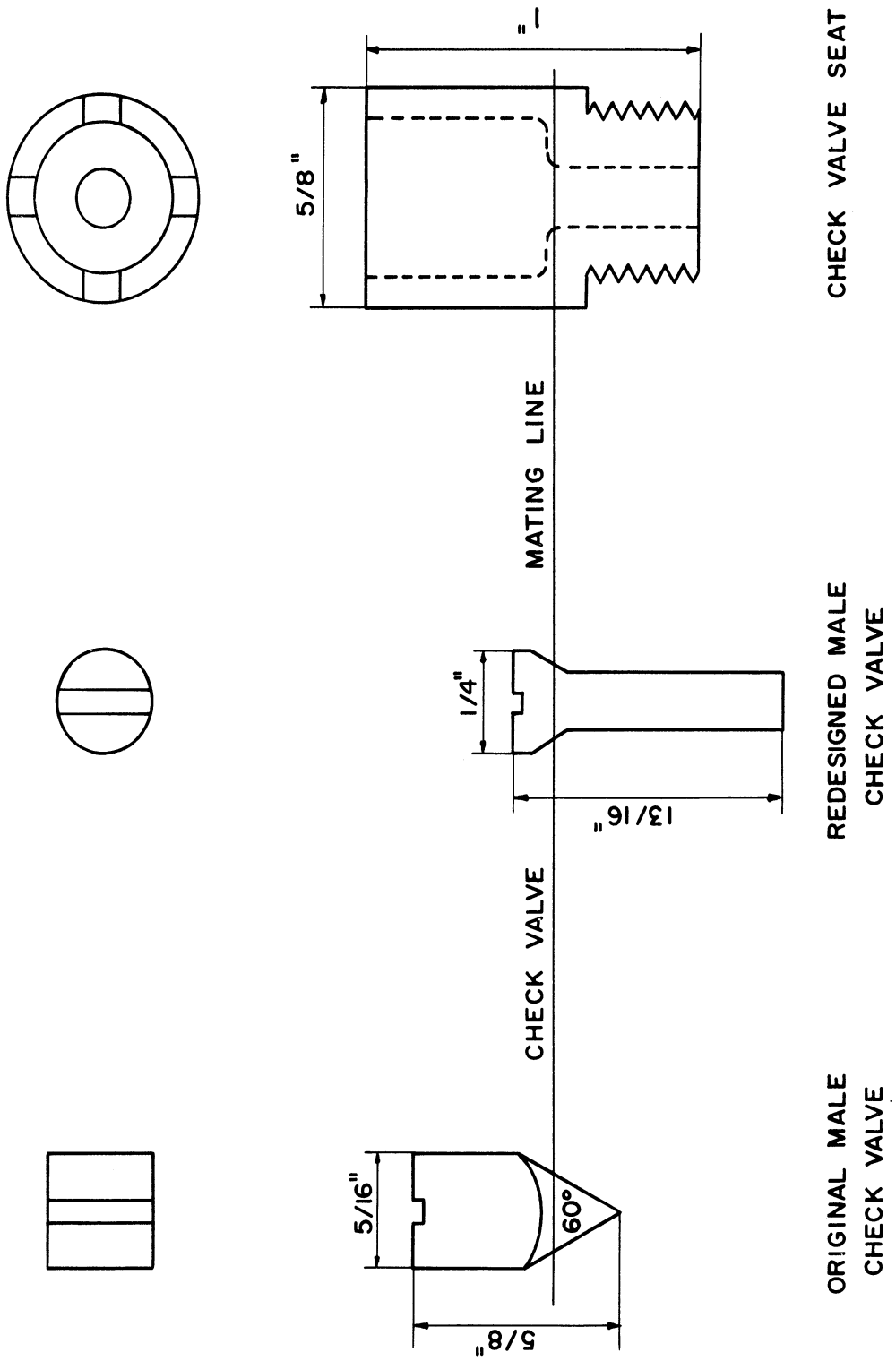

Figure 5. Check Valve Assembly for Hills-McCanna Pump

formed is an extremely narrow conical surface, but was found to give very dependable service in contrast to erratic performance when wide contact seats were made.

With these modifications, the pump performed most successfully over the entire range of flow rates used, that is, 0.30 to 18 cc/min. After steady-state operation was completely established, the pumping rate seldom fluctuated by more than $\pm$ 1%.

Reactor

The reactor designed by Sleipcevich (23) and fabricated of 19-9 W-Mo stainless steel was used for this investigation. The details of this design, which are not particularly relevant to the present study, may be obtained from the reference cited above. Briefly, the reactor provides an annular cross-section, 3/4" x 1/4", (a 1/4" diameter thermowell extends the entire length of the reactor), in which catalyst beds of up to 30" in length may be packed.

The necessity of isolating the resin from the stainless steel walls became apparent when it was found that the cation resin exchanged its hydrogen for metal ions from the steel walls at a relatively rapid rate at the higher temperatures used. The first attempt to stop this affect was to insert a spiral wrap of 0.0025" thick Teflon tape around both the 3/4" diameter reactor inside wall and around the 1/4" diameter thermo-

well tubing. While this procedure greatly decreased the ion exchange rate, it was not completely effective due to unavoidable gaps in the spiral wrapped linings. Eventually all ion exchange with the resin was eliminated by obtaining tantalum liners for the reactor. The dimensions of the three liners are as follows:

30" x 3/4" O.D. x 0.020" wall thickness (for reactor inside wall)
34 1/16" x 1/4" I.D. x 0.010" wall thickness (for thermowell)
2 1/16" x 5/16" I.D. x 0.010" wall thickness (for outlet section below resin).

The three tantalum liners are shown on Figure 6. The tubing fitted so tightly that in each case a small amount of grinding was necessary before the liners could be inserted. As anticipated, the tantalum was completely inert to the resin environment.

In order to obtain high mass velocities for some runs without using inconveniently high feed rates, the reactor inside diameter was reduced by insertion of pyrex liners. For this purpose two pieces of pyrex tubing, 17 mm and 14 mm O.D., with 1.2 mm walls, were cemented into one piece by drawing #31 Sauereisen cement into the small annular clearance between them. By-passing of fluid between the pyrex and tantalum liners was prevented by cutting the 17 mm diameter pyrex tubing one inch shorter than the 14 mm tubing to which it was cemented. By inserting the flush end of the pyrex tubing to the bottom of

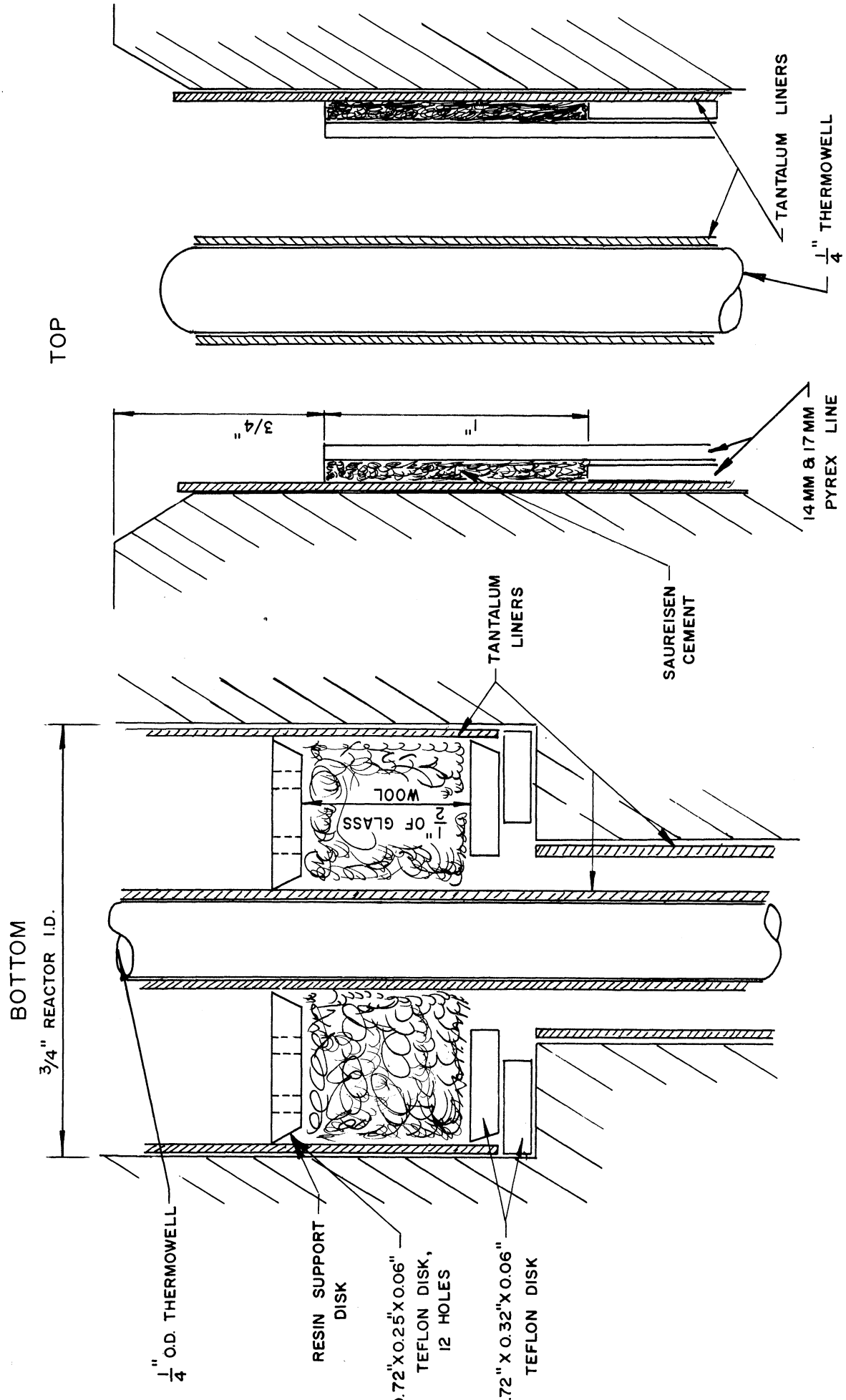

Figure 6. Reactor Sections Showing Tantalum and Pyrex Liners.

the reactor, an annular space 1.2 mm wide x 25 mm deep was left at the top. This annular space was then solidly filled with Saureisen #31 cement with 25% of the silicate binder replaced for extra strength by pulverized glass wool. The position of the pyrex liners is illustrated in Figure 6.

Reactor Temperature Control and Measurement

The original method of reactor temperature control by means of heating the insulated enclosure around the reactor was replaced by a method more appropriate to the present study. The reactor was wrapped directly with coils of insulated resistance wire having the following specification:

Manufacturer	Driver-Harris Co.
Type	No. 33 Alloy (97% Ni, 3% Si)
Size	36 gage
Insulation	Fiberglass
Ohms per foot	7.5 at 75°F; 9.1 at 300°F

The reactor was wound in five separate sections with this heating wire, with each section controlled by a separate voltage regulator. The section of reactor covered by each winding is listed below:

Reactor section	Heating coil, ohms (cold)
Reactor inlet tubing	3 coils in parallel, 180 Ω each
Top 11" of reactor	345 Ω

Middle 9" of reactor	235 Ω
Bottom 9" of reactor	235 Ω
2" section below catalyst	215 Ω

The large heat capacity of the heavy-walled reactor served to even out any local fluctuations of outside surface temperature so that this method of temperature control was quite satisfactory.

A chromel-alumel thermocouple with glass fiber insulation was calibrated over the range of temperatures involved and was used as a travelling thermocouple in the reactor thermowell.

IV MATERIALS

Chemicals

A 28 gallon cylinder of butene was provided through the courtesy of Phillips Petroleum Company. The analysis supplied with this cylinder was determined on their infra-red spectrometer.

	mol %
isobutane	0.0
isobutylene	0.0
butene-1	0.0
butadiene-1,3	0.0
n-butane	2.9
trans-butene-2	48.0
cis-butene-2	49.1
neopentane	0.1
	100.0

For the few runs containing sec-butyl alcohol in the feed, the alcohol used was Eastman-Kodak reagent grade #903. The small amount of water contained in this material is of no consequence since the aqueous feed solution was made up and analyzed by density.

Cation Exchange Resin

The Dow Chemical Company supplied various grades of Dowex-50, their trade-name for monosulfonated polystyrene cross-linked with divinylbenzene. Most of this resin was the special grade which is sulfonated under conditions giving a particularly uniform product, which is also lighter in color due to less charring of the organic polymer base. Resin produced in this way carries the extra designation, Dowex-50W.

The commercial size ranges of resin produced by The Dow Chemical Company were used for most of the present study. Within each of the size ranges used (50 - 100, 100 - 200, and 200 - 400 mesh), however, about 5 - 10% of the resin at either end of the size distribution was removed. For the larger sizes this narrowing of the distribution of sizes was accomplished by wet screening, and for the smaller sizes by elutriation.

After this operation, the resin was acid-washed to remove any trace of metal ions. This is particularly important after the resin has been in contact with the copper screens. Finally, the resin was washed with distilled water until the effluent water was nearly neutral, as indicated by a pH meter.

The specifications for each charge of resin used is listed in Table I.

Table I

Cation Exchange Resins Used

Resin Designation	Weight gms (anhyd.)	Mesh Size	% DVB	Dowex-50 or -50W
L	59.9	80 - 100	8	50
M	52.5	80 - 100	8	50
N	55.1	100 - 200	12	50W
O	51.8	100 - 200	8	50W
P	51.6	100 - 200	8	50W
Q	57.6	200 - 400	8	50
R	16.53	100 - 200	8	50W
S	16.10	50 - 100	8	50W
T	4.93	100 - 200	8	50W

V EXPERIMENTAL PROCEDURE

Analytical Methods

Overall analysis scheme

The overall measurement scheme must be taken into account in choosing the analytical methods to be used. The feed rate and composition are known to a high degree of precision. Upon reduction of pressure, the reactor product, which in most cases consists of two liquid phases, separates into an aqueous alcohol liquid and a butene-rich gas. The gas and liquid products are separated at atmospheric temperature and pressure in a manner which assures their being in equilibrium. The gas stream contains an amount of sec-butyl alcohol and water proportional to their vapor pressure over the liquid product. Similarly butene is dissolved in the liquid product to the extent of its solubility at one atmosphere. The total reactor product is calculated from a combination of the rates and compositions of the two product streams.

Two alternate calculation methods were used to determine the total reactor product. One solution was graphical and represented the solution of the two equations:

(1) the equation of all possible reactor product compositions consistent with the feed used and the reaction stoichiometry, and,

(2) the equation of all reactor product compositions which could give the gas and liquid product compositions obtained.

When large scale graph paper is used, the intersection of the lines corresponding to the above two equations gives a precise stoichiometric reactor product composition, which directly determines reaction rates and conversions. The other method was a numerical calculation of the total alcohol produced. Precision of results and convenience determined the choice between these two methods for any run.

Butene in the liquid product

For most of the experiments, the composition of the liquid product is the most important product measurement required. Since measurement of the density of the aqueous alcohol liquid product permits rapid determination of composition with a high degree of precision, this method of analysis was selected. However, because butene at one atmosphere is soluble in the aqueous butyl alcohol solutions, it was necessary to consider this effect. Since no data were available for this system, measurements were made of the solubility of butene at 25°C, 1 atm, in sec-butyl alcohol solutions of various concentrations. These values, adjusted to the average local barometric pressure, 744 mm, are listed in Table II.

Table II

Binary composition wt. % sec-butyl alcohol		100%	81.7%	11.56%
Butene saturated	A	90.0	75.44	11.55
ternary compo-	W	--	16.80	88.36
sition, wt. %	B	10.0	7.76	0.09

It was also observed that binary compositions just slightly above the 11.56% butyl alcohol solution gave two liquid phases when saturated with butene. Thus the 11.56% solution, when saturated with butene, may be taken as a close approximation to the composition of one of the equilibrium phases of the three phase invariant at 25°C and 744 mm. These phase relations are illustrated on Figure 8, p 42. For alcohol concentrations less than 11.5%, therefore, single phase liquid products were obtained. The butyl alcohol content of these samples was calculated from a density determination on the butene saturated liquid product, with an allowance for the effect on density of the small amount of butene dissolved in such dilute solutions. For alcohol concentrations between the 11.5% limit above, and 18.6%, which is the lower solubility limit in the alcohol-water binary system, a two-phase butene satured liquid product was obtained. This two-phase liquid was subjected to a rapid differential vacuum distillation, by which it was converted to a butene-free single phase suitable

for analysis by density.

Differential vacuum distillation

While these procedures were quite satisfactory for this range of liquid product compositions, a more difficult problem was presented by the concentrated alcohol products obtained from some runs. For liquid products in the range 75 - 80 wt. % butyl alcohol, the amount of butene to be removed is such that the removal process can cause considerable change in the alcohol/water ratio. This change can be minimized and standardized by performing a Rayleigh distillation, that is, a differential distillation in which the vapor removed is always in equilibrium with the solution remaining. For the present work it seemed advantageous to conduct the distillation at 25°C; the pressure, therefore, decreases from atmospheric at the beginning to a final pressure a few millimeters above the vapor pressure of the butene-free liquid.

In order to calculate the change in butyl alcohol/water ratio which results from the differential vacuum distillation, certain required physical data which were not available in the literature were determined. A few points on the alcohol-water vapor-liquid equilibrium curve at 25°C were measured. These data are plotted in the appendix, Figure 19 . The equilibrium values were obtained by careful material balance measurements on an alcohol-water solution distilled at 25°C. The vapor pressure of the sec-butyl alcohol-water binary at 25°C

as a function of composition was also measured, and may be found in the appendix, Figure 18 . With these data available, it was then possible to establish distillation conditions and calculate the butene/water ratio correction. These calculations are summarized in Appendix A . This correction factor was calculated as a function of concentration and final pressure, and is plotted in the appendix, Figure 20 . Briefly, the results of these calculations indicate that the weight ratio, alcohol/(alcohol + water), is increased by about 0.35 weight percentage units when the butene is removed from solutions in the range 75 - 80 wt. % sec-butyl alcohol. This correction applies for a final pressure 7 mm. mercury above the vapor pressure of the alcohol-water binary.

In order that these theoretical corrections may be applied, the distillation apparatus must be designed so that the vapor removed is sufficiently close to being in equilibrium with the liquid remaining. While this condition could be satisfied by conducting the distillation very slowly, practical considerations require a reasonably rapid operation. In this case the rate of pressure reduction was set at 30 - 50 mm./min., so that a distillation could be completed in about 20 minutes. The rate of pressure reduction was controlled by connecting the vacuum pump to the distillation apparatus through a set of capillary tubes operated in parallel. The various sizes of capillary tubes were connected into the flow-path according to a standardized time sequence in order to maintain the pressure reduction rate within the 30 - 50 mm/min. range. With

the vapor removal rate fixed, the remaining variable is the degree of agitation during the distillation. Here, the problem of obtaining sufficient agitation inside a vacuum distillation flask presents considerable difficulty. Several methods were tried before one was found which gave distillation corrections which were neither erratic nor larger than the theoretically calculated ones. The method finally adopted involved clamping the vacuum distillation flask to an incompletely restrained framework onto which an electric motor carrying a small eccentric load was also clamped. This procedure kept the liquid in a state of violent agitation and, as a result, the experimentally measured distillation corrections for known solutions agreed exactly with the theoretical corrections. The apparatus was completed by a water bath to control the distillation temperature at 25°C. Also, flasks were connected in parallel to allow four distillation samples to be run simultaneously, thus reducing the total distillation time required. A picture of the distillation apparatus is shown in Figure 7.

Density determination

Although the pycnometer method is most commonly used for density determinations, the buoyancy method was chosen for this study because it allows more rapid determinations. By using an accurately calibrated sinker, and making the weighings on a good analytical balance with careful temperature control, it is possible to make rapid density determinations which are

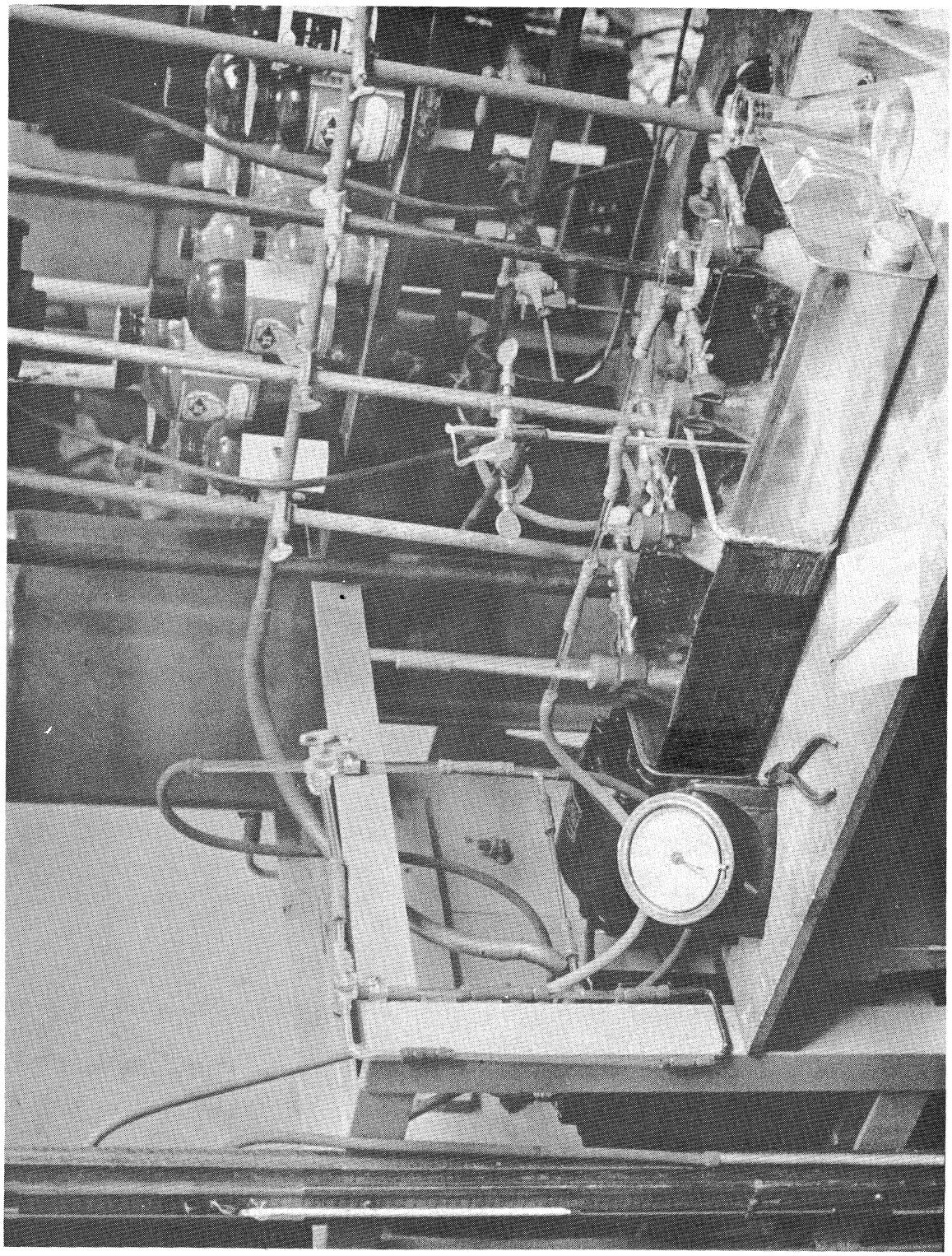

Figure 7. Differential Vacuum Distillation Apparatus.

accurate to about ± 0.00002 g/ml. This density range corresponds to a concentration range of about ± 0.013 weight % sec-butyl alcohol. At times, however, it was found that the precision was not achieved. It was only fairly late in the research that it was discovered that this occasional aberrant behavior of the sinker did not occur if it was washed with a mild detergent solution rather than with reagent grade solvents as had previously been the practice. The calibration of the sinker in water gave the volume as 5.01183 ± 0.00012 ml.

The data of Clough and Johns (6) was used to relate densities to concentrations for sec-butyl alcohol-water mixtures. Rapid calculations were facilitated by preparation of working graphs of alcohol concentration against grams weight on the balance, with corrections for temperature, distillation, and butene solubility all expressed in terms of grams weight.

Gas product analysis

Since the amount of sec-butyl alcohol and water which leave in the gas product are proportional to their corresponding vapor pressures over the liquid product, the accuracy of the gas product analysis is generally of much less importance than that of the liquid product. The gas analysis was therefore calculated from the alcohol-water binary vapor pressure and vapor-liquid equilibrium data at 25°C. These calculations are summarized in Appendix B.

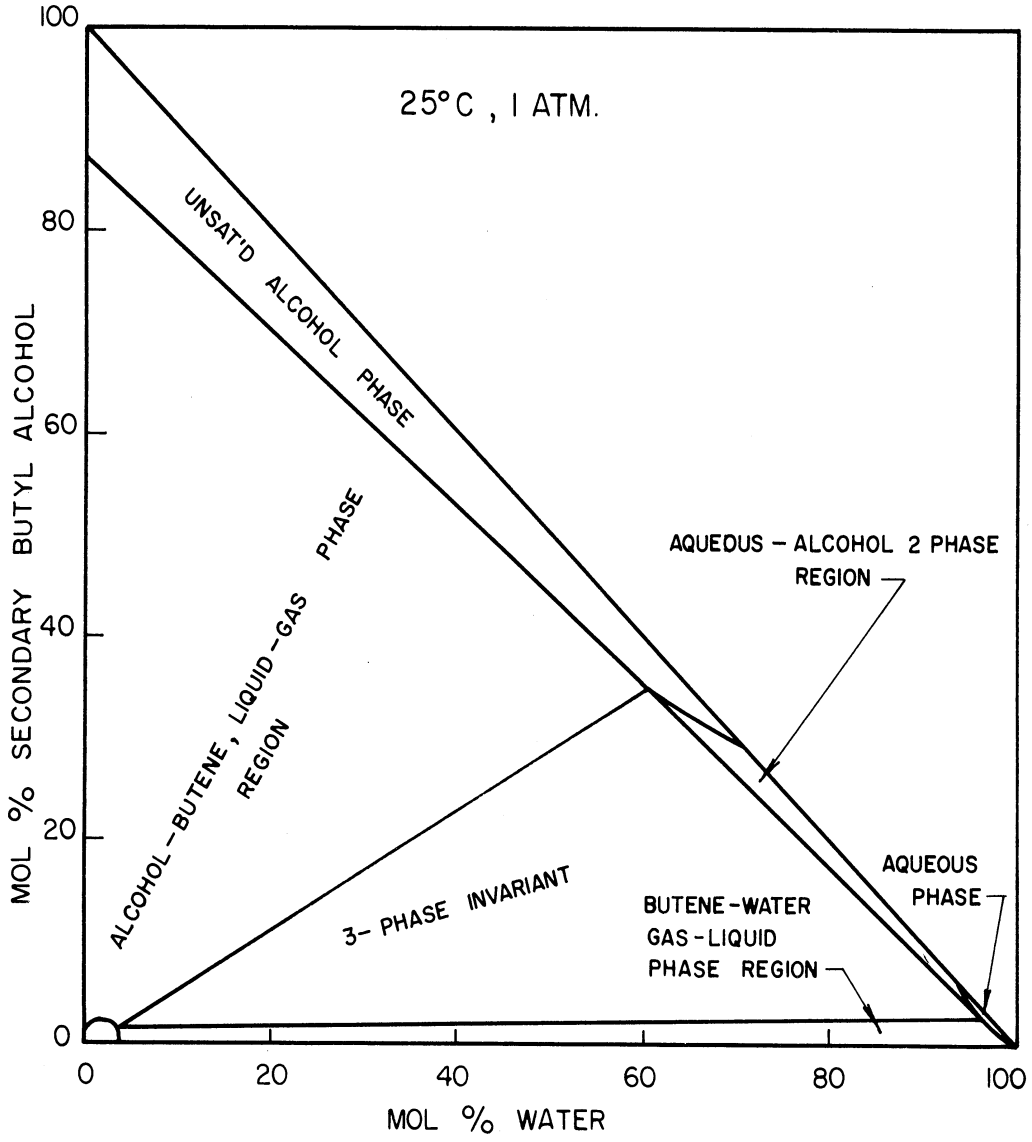

Figure 8. Ternary Phase Diagram at 25°C, 1 Atmosphere.

Phase diagram for product gas and liquids

The various phase equilibrium data at 25°C and 1 atm. which have been discussed in this section may be conveniently represented on a butene-water-sec.-butyl alcohol equilibrium phase diagram. The only significant point which has not been either measured or estimated is the alcohol-rich liquid phase at the three-phase invariant. From other measurements it is believed that this point lies at about 37 mol % alcohol/(alcohol + water). This phase diagram is included in the appendix, Figure 8.

Reactor Operation

Before the reactor was placed in the operating position, it was charged with water saturated ion exchange resin. The reactor closures were made first at the bottom and then at the top so that no air was trapped in the system. All reactor feed lines were also flushed just prior to being connected in order to eliminate any trapped air. The pneumatic reactor pressure control valve was loaded with nitrogen or helium at the desired reactor pressure.

After flow was established through the reactor, some time usually elapsed before the desired feed rates and temperature were obtained. The gage readings of the butene and aqueous feed cylinders were taken at appropriate intervals to accurately determine feed rates. Similarly, reactor product gas and liquid rates were determined and the reactor temperatures recorded. An operating period at steady-state conditions was required

before the reactor product reached the corresponding equilibrium value. Since the method of analysis used was rapid, both the steady-state and the unsteady-state samples were usually analyzed, thus giving greater confidence in the final values. From this procedure it was observed that the reactor product rapidly approached the steady-state composition after the operating conditions became constant. Normally a given set of conditions was maintained until two or three samples of the steady-state liquid product were collected. The variation in results from these duplicate runs therefore reflects both analytical errors and variation in reactor operation. Since the minimum sample size required for the density determination was about 30 ml, the time at steady-state required for each sample varied from a few minutes to about an hour.

Following the completion of a series of runs, the resin was removed by fluidizing it into the large end of a pipette which was fitted with a glass tubing extension of sufficient length to reach the bottom of the reactor. This operation was carried out so as not to lose any of the resin, which was then dried and weighed. In order to get anhydrous weights of resin, the small amount of water remaining in the resin at equilibrium in the drying oven was estimated using water-sorption data of Gregor (12) and Pepper (20). The relative humidity in the oven at 110°C was determined by assuming the absolute humidity to be the same as that of the surroundings. All resin samples were dried together at the end of the experimental program so that any errors would affect samples equally.

VI RESULTS

The experimental results relating to the measurement of hydration rates for normal butene in the continuous catalytic process are presented first. The experimental data are summarized in Tables III and IV.

The range of variables studied was as follows:

Temperature	115 - 145°C
Resin size	50 - 400 mesh
Resin crosslinkage	8% and 12% divinylbenzene
Superficial liquid velocity	40 - 1100 cm/hr.
Resin weight, anhydrous	4.9 - 60 gms.
Butene conversion (hydration	12.2% max.
Alcohol conversion (dehydration)	30.7% max.
Feed composition	
Mol % butene	20% - 82%
Mol % alcohol	0% - 25%

Liquid Phase Mass Transfer Effect

Since it was necessary to obtain rates which would be independent of any liquid phase mass transfer effect, six runs were made to determine the required operating conditions. The usual procedure for this purpose is to characterize flow

EXPERIMENTAL RESULTS FOR DETERMINATION OF REACTION RATES

TABLE III

Run	Resin[1]	Temp. °C	Feed Rate W gm/min	Feed Rate B gm/min	Fv[2] ml/hr	Feed Composition Ratios mol % W	(B/W)v[2] vols/vol	Space Velocity hr^{-1} gm/mol/hr	Liquid Product Composition wt % A/AW in Duplicate Runs				Liquid Product Rate A gm/min	Liquid Product Rate W gm/min	Equilibrium Flash Gas Prod. A mol %	Equilibrium Flash Gas Prod. W mol %	Equilibrium Flash Gas Prod. B mol %	Gas Prod. Rate A gm/min	Gas Prod. Rate W gm/min	Total Product A gm/min	Total Product W gm/min	Mat. Bal on W %	% Convn. of B	Integral Reaction Rate mols/hr/gm H R x 10^3
49,a	N	140	5.29	3.71	901	81.6	1.63	2.55	0.55	0.67			0.0313	5.11	0.097	4.51	95.4	0.0050	0.056	0.0363	5.17	101.4	0.74	0.534
69,a	P	140	0.551	0.412	97.5	80.6	1.74	22.7	8.54	8.44			0.0516	0.556	1.11	3.72	95.2	0.0057	0.005	0.0573	0.561	104.5	10.5	0.90
87,a		115	4.50	3.55	740	79.8	1.60	0.88	0.35	0.325			0.0150	4.43	0.045	3.5	96.5	0.0022	0.041	0.0172	4.47	100.3	0.367	0.84
88,a,b	R	120	4.49	3.61	758	79.5	1.66	0.884	0.55	0.56	0.52		0.0248	4.45	0.072	3.6	96.3	0.0035	0.043	0.0283	4.49	101.3	0.594	1.39
89,a,b		125	4.49	3.61	773	79.5	1.69	0.884	0.76	0.90	0.77		0.0356	4.36	0.108	3.7	96.2	0.0053	0.044	0.0409	4.40	100.0	0.858	2.00
90,a,b		130	4.49	3.61	788	79.5	1.74	0.884	1.21	1.205	1.105		0.0501	4.30	0.156	3.7	96.1	0.0076	0.044	0.0577	4.34	97.3	1.21	2.82
96,a,b,c	S	130	4.58	3.51	780	80.2	1.65	0.848	1.00	0.98	1.01	1.00	0.0454	4.50	0.133	3.7	96.2	0.0064	0.043	0.0517	4.54	99.5	1.115	2.60
97,b		130	1.51	4.62	736	50.4	6.62	0.494	0.76	0.74			0.0112	1.48	0.100	3.65	96.25	0.0063	0.056	0.0175	1.54	98.2	0.287	2.88
98,a,b	T	135	4.00	3.58	773	77.7	1.99	0.287	0.49	0.52	0.53		0.0209	4.06	0.068	3.6	96.3	0.0033	0.043	0.0242	4.10	102.5	0.513	3.98
99,a,b		140	4.48	3.48	812	80.0	1.79	0.265	0.68	0.75	0.75		0.0323	4.41	0.097	3.6	96.3	0.0046	0.041	0.0369	4.45	99.5	0.803	6.05
100,a,b		145	4.52	3.45	840	80.3	1.85	0.263	1.085	1.075	1.125		0.0490	4.42	0.146	3.7	96.2	0.0068	0.042	0.0558	4.46	99.0	1.225	9.17

TABLE IV

Run	Resin[1]	Temp. °C	Feed Rate A gm/min	Feed Rate W gm/min	Feed Rate B gm/min	Fv[2] ml/hr	Equiv. Binary Feed mol % W	Feed Ratio[2] (B/W)v vols/vol	Space Velocity hr^{-1} gm/mol/hr	Liquid Product Composition, wt % A/AW Duplicate Runs			Average	Stoichiometric Reactor Product A mol %	Stoichiometric Reactor Product W mol %	Stoichiometric Reactor Product B mol %	Mols Convd. Mol Feed x 100	% Convn. of B	Integral Reaction Rate mols/hr/gm H R x 10^3
25,a,b		130	0.763	0.111	1.40	233	31.9		24.0	83.83	83.55	83.00	83.46	18.8	19.0	62.2	-5.15	-8.5	-2.03
26,a,b	L	140	0.736	0.107	1.30	224	32.3		25.5	76.85	76.70	76.10	76.55	16.3	21.2	62.5	-7.78	-13.1	-3.16
27,a,b		110	0.724	0.105	1.32	213	31.8		24.0	90.71	89.52	88.84	89.69	26.9	13.5	59.6	1.63	2.7	0.67
28,a,b		120	0.768	0.112	1.35	224	32.3		24.4	87.28	87.34	86.94	87.18	24.5	15.7	59.8	-0.68	-1.1	-0.23
59,a		125		1.95	1.55	334	79.7	1.67	6.35	4.29	3.99		4.14	0.893	79.46	19.65	0.952	4.69	1.47
60,a,b	O	130		2.03	1.52	341	80.6	1.62	6.17	4.89	4.96	4.87	4.91	1.076	80.42	18.5	1.13	5.80	1.82
61,a,b		135		1.99	1.57	355	79.8	1.75	6.23	5.14	5.14	5.22	5.17	1.127	79.49	19.38	1.17	5.80	1.88
62,a		140		2.00	1.58	366	79.7	1.83	6.19	5.54	5.03		5.28	1.150	79.40	19.45	1.19	5.88	1.94
64,a		115		0.523	0.410	85.7	79.8	1.59	23.6	5.83	4.53		5.03	1.093	78.43	20.48	1.15	5.69	0.485
65	P	120		0.502	0.412	86.0	79.1	1.69	23.1	7.70			7.70	1.723	78.85	19.43	1.90	9.12	0.777
66,a		125		0.535	0.417	90.2	80.0	1.64	22.0	8.19	8.25		8.22	1.861	79.52	18.62	2.04	10.2	0.87
67,a		130		0.497	0.412	89.0	79.0	1.79	23.3	8.58	8.94		8.76	1.983	78.51	19.51	2.17	10.3	0.89
77,a,b		130		2.02	1.56	346	80.1	1.67	6.85	1.64	1.45	1.47	1.52	0.320	80.00	19.68	0.34	1.69	0.49
78,a	Q	130		0.678	2.41	377	46.7	7.69	11.9	7.04	6.96		7.00	1.138	46.10	52.76	1.28	2.4	1.085
79,a		115		3.15	10.9	1590	47.4	7.28	2.59	0.50	0.41		0.445	0.064	47.37	52.57	0.074	0.14	0.28
80		115		9.17	7.06	1465	80.2	1.62	1.51	0.12			0.12	0.025	80.18	19.80	0.026	0.13	0.17

(1) See Table I for significance of symbols

(2) Volumes at reactor inlet conditions

conditions by the Reynolds modulus, then measure the reaction rate constant for a series of runs at increasing values of the Reynolds modulus. Flow conditions corresponding to negligible liquid phase mass transfer resistance can then be selected by operating at values of the Reynolds modulus above the range in which the rate constant is dependent on this modulus. This principle was used, but in a slightly different form for this study. The characterization by a Reynolds modulus of two-phase fluid flow over packed beds involves theoretical problems which have not yet been completely solved. For the present purpose, however, it is satisfactory to use a modified Reynolds modulus defined as

$$Re' = \frac{D_p F_v}{A} .$$

where D_p = average resin diameter as charged

F_v = total liquid feed rate, at reactor temperature, cc./hr., and

A = reactor cross-sectional area, $cm.^2$.

(The ratio F_v/A is sometimes referred to as the superficial velocity, cm./hr.)

Also, since it is not possible in the present study to calculate a reaction rate constant, k, a different criterion variable was selected. This selection was based on the principle that for a flow reactor operated with a two-liquid phase feed, the reaction rate will not be affected by a change in the ratio of the two liquid phases, provided there is

negligible liquid phase mass transfer resistance, and that all other conditions are held constant. Conversely, one would expect variation in reaction rate with variation in the proportions of the two liquid phases, unless there is negligible liquid phase mass transfer resistance.

The experimental approach developed from the above considerations involved making a series of three pairs of runs, with a large difference in the butene/water phase ratio as the only variable within each pair. A significantly different Reynolds modulus was selected for each of the three pairs of runs. For each pair, the ratio of the reaction rate for the high butene/water feed to the rate for the low butene/water feed was taken as the criterion of the relative importance of liquid phase mass transfer resistance. The pertinent values from this series of runs are given below in Table V.

Table V

Run	D_p cm.	F_v cc/hr	A cm^2	r g mols / (hr)(gm HR)	$(B/W)_v$	r_2/r_1*	Re'
77	0.0056	346	2.175	0.492	1.67		
78	0.0056	377	2.175	1.085	7.69		
		360 ave.				2.2	0.93
80	0.0056	1465	2.175	0.174	1.62		
79	0.0056	1590	2.175	0.283	7.28		
		1530 ave.				1.6	3.9
90	0.011	788	0.691	2.82	1.74		
97	0.011	736	0.691	2.78**	6.62		
		760 ave.				1.0	12.1

* r_2 refers to the run at high butene/water ratio

r_1 refers to the run at low butene/water ratio

** Adjusted for slight deviation in space velocity.

It will be noted from this table that liquid phase mass transfer resistance can be neglected at values of $Re' = 12$.

Initial Reaction Rates

For the hydration of normal butylene, represented as

$$n\ C_4H_8 + H_2O = C_4H_9OH,$$

a generalized differential reaction rate equation in terms of thermodynamic activities may be written as follows:

$$r = k\left[(a_B)^a\,(a_W)^b - \frac{(a_A)^c}{K_a}\right] \quad \frac{\text{g mols A}}{(\text{hr})(\text{gm HR})}$$

The bracketed term is the kinetic driving force. For a flow reactor at steady state, the reaction rate may be related to a material balance over a differential length of the reactor according to the equation

$$r\,dW = -F_m\,dn_A \quad \text{g mols A/hr.}$$

$$\text{or} \quad r = -\frac{dn_A}{d(W/F_m)} \quad \frac{\text{g mols A}}{(\text{hr})(\text{gm HR})}$$

These differential equations may, with appropriate substi-

tutions, be integrated; or, conversely, integral reaction rates may be measured directly and represented as

$$r_I = - \frac{\Delta n_A}{\Delta (W/F_m)} \frac{\text{g mols A}}{(\text{hr})(\text{gm Hr})}$$

The performance of a flow reactor operated at constant temperature with a constant composition feed containing no alcohol will be considered. As the reciprocal space velocity, W/F_m, is decreased, the alcohol content of the reactor effluent decreases, approaching zero, and the butene and water composition of the product increase, approaching the feed composition. For a particular feed composition and temperature, the kinetic driving force, therefore, approaches a maximum as the reciprocal space velocity approaches zero. The corresponding maximum reaction rate is defined as the initial reaction rate. In the special case of a binary feed consisting of two almost completely immiscible liquids, the proportions of the two phases cannot affect the initial reaction rate, which therefore becomes a function of temperature only. It follows that the initial reaction rate may be obtained for a given temperature by plotting the integral reaction rates against reciprocal space velocity, and extrapolating the rate curve to zero. In order that the initial reaction rates determined in this way do not include any error due to mass transfer resistance the space velocities used must include values for which the liquid phase mass transfer resistance may be neglected. Satisfactory space velocities have been determined

in the previous section.

In this study runs were made at a number of space velocities for seven temperature levels from 115° to 145°C. The integral reaction rates calculated for each of these runs are listed in Tables III and IV, and are plotted against reciprocal space velocity with temperature as a parameter in Figure 9. Each isotherm is extrapolated back to $W/F_m = 0$ to obtain the initial reaction rate for that temperature. The crossing of isotherms at the lowest space velocities used is not due to experimental error but is caused by the close approach to equilibrium under these experimental conditions. This effect will be discussed further when the equilibrium measurements are presented. Before the reaction rate data can be interpreted further, the effect of resin size must be evaluated.

Effect of Resin Size

The efficiency function method developed by Saletan and White (21) to allow for the effect on reaction rate of the resin phase diffusional resistance is used in this study to evaluate the effect of variation in resin size. As described earlier, the efficiency function, ϕ, plotted on Figure 9 represents the ratio of the volumetric average reaction rate to the reaction rate at the surface of the resin bead. It may be represented as an analytic function of the resin radius, R, and the penetration function τ. The penetration function, τ, is theoretically dependent on both temperature and com-

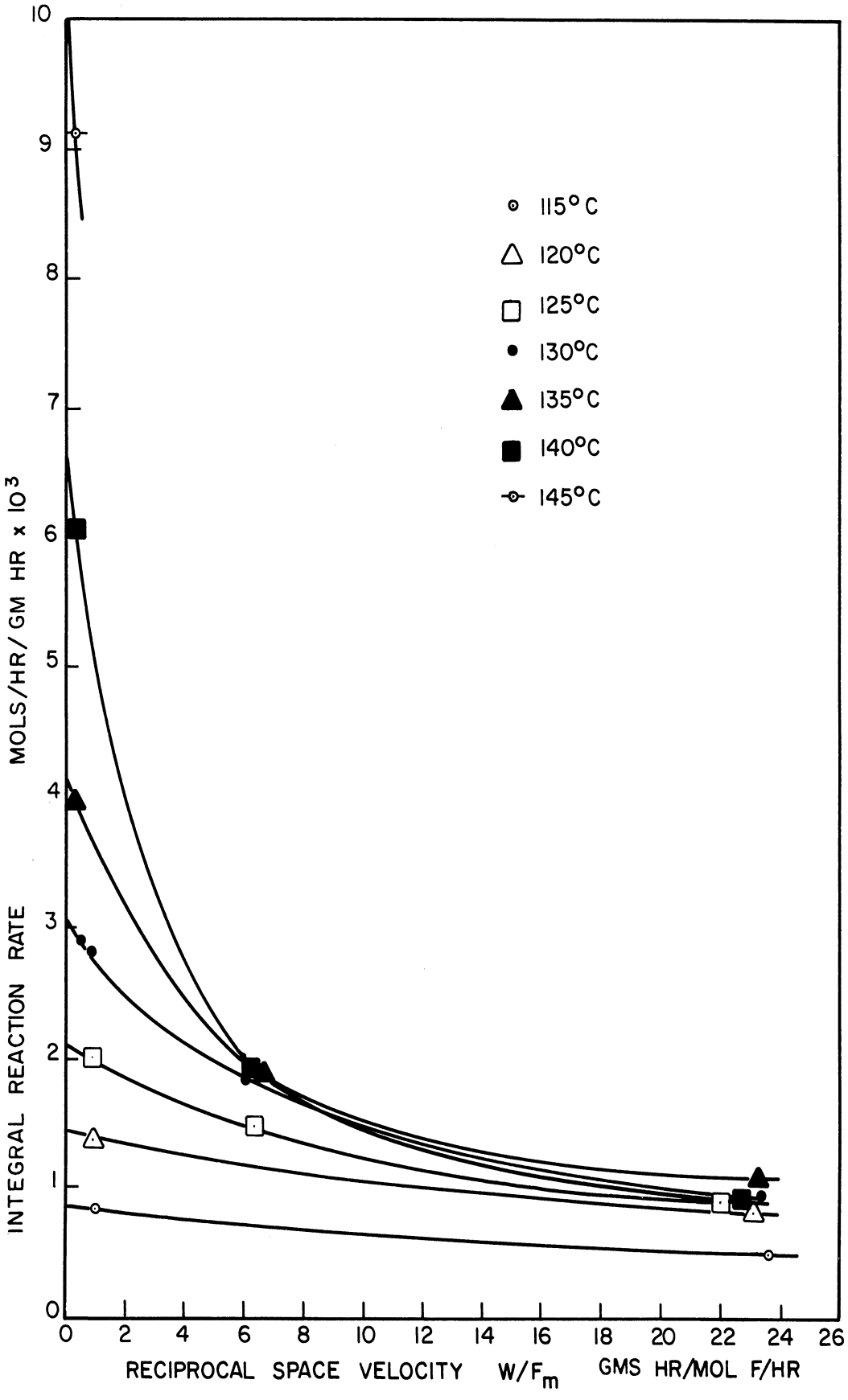

Figure 9. Effect of Temperature and Space Velocity on Integral Reaction rate.

position. In practice, however, both Saletan (21) and Barker (3) found only a slight dependence of ϕ on temperature, and Klein (15) found no measurable temperature dependence of ϕ for the reaction system analyzed by him. Also, in the consideration of initial reaction rate data for the butene hydration system, it has already been noted that the liquid phase composition is not a variable. For this study, therefore, the efficiency function, ϕ, may be assumed to be a constant, even though the exact value of the function cannot be determined. Thus for initial reaction rate data, ϕ may be taken as a function of only resin radius, R.

In order to determine the actual value of ϕ which applies to all the initial reaction rate data already presented, two series of runs, involving seven runs in all,were made. The runs were performed under nominally identical conditions, except that for one series the resin radius was double that used in all the runs for the determination of initial reaction rates. The pertinent results from this series of runs are given below in Table VI. Since the space velocity was slightly different for the two series of runs, the results of run 90 have been adjusted to the same space velocity as run 96. The adjusted results are designated as run 90'.

Table VI

Run	Temp	HR radius	W/F_m $\frac{(\text{gms HR})(\text{hr})}{\text{g mol feed}}$	r_I $\frac{\text{g mols}}{(\text{hr})(\text{gm HR})}$
90	130	0.011	0.884	2.82×10^{-3}
90'	130	0.011	0.848	2.83×10^{-3}
96	130	0.022	0.848	2.60×10^{-3}

It can be seen from these values that doubling the bead radius from that used in the determination of initial reaction rates has caused a decrease in reaction rate of only 8.1%. By matching this ratio of efficiency functions (i.e. $\phi_2/\phi_1 = 0.919$ for $R_2/R_1 = 2$) to the plot of ϕ versus R, Figure 3, p. 17, it can be determined that ϕ_1, the value pertaining to the initial reaction rate measurements, must be 0.973. The initial reaction rates, given by the intercept at $W/F_m = 0$ on Figure 9 correspond therefore to a resin of 97.3% volumetric efficiency. From the definition of ϕ it follows that, for the cation exchange resin catalyst used, one may obtain an initial chemical reaction rate which is independent of any resin phase diffusional resistance by dividing the zero intercept values from Figure 9 by $\phi = 0.973$. These intercepts and the corresponding pure chemical reaction rates are given in Table VII.

Table VII

Temperature °C	Initial Reaction Rate using 100-200 mesh resin $\frac{\text{g mols A}}{(\text{hr})(\text{gm HR})} \times 10^3$	Initial Chemical Reaction Rate $\frac{\text{g mols A}}{(\text{hr})(\text{gm HR})} \times 10^3$
115	0.87	0.89
120	1.45	1.49
125	2.10	2.16
130	3.05	3.13
135	4.13	4.24
140	6.75	6.93
145	10.0	10.3

An expression can be written for the initial hydration rate data following the form commonly used for liquid phase reactions, that is,

$$r_i = k\, C_{B_i}^{\ a}\, C_{W_i}^{\ b} \qquad (C_{A_i} = 0),$$

where the temperature dependence of the reaction rate constant, k, is given by the Arrhenius equation,

$$k = A \exp(-E/RT).$$

Since for the butene hydration reaction the two components of the feed are almost completely immiscible, the initial reaction rate is not dependent on feed composition. The initial reaction rate expression, then, reduces to

$$r_i = \text{constant} \times \exp(-E/RT).$$

It follows that a plot of the logarithm of initial reaction rate, r_i, against reciprocal absolute temperature, 1/T, will give a straight line, the slope of which equals the activation energy, E.

The initial chemical reaction rates from Table VII have been plotted in this manner on Figure 10. Since the initial rate data can be satisfactorily represented by a straight line on this plot, the energy of activation, (E = 24,800 cal/mol), was calculated from its slope. It also follows from this figure that the constant in the initial reaction rate expression, which

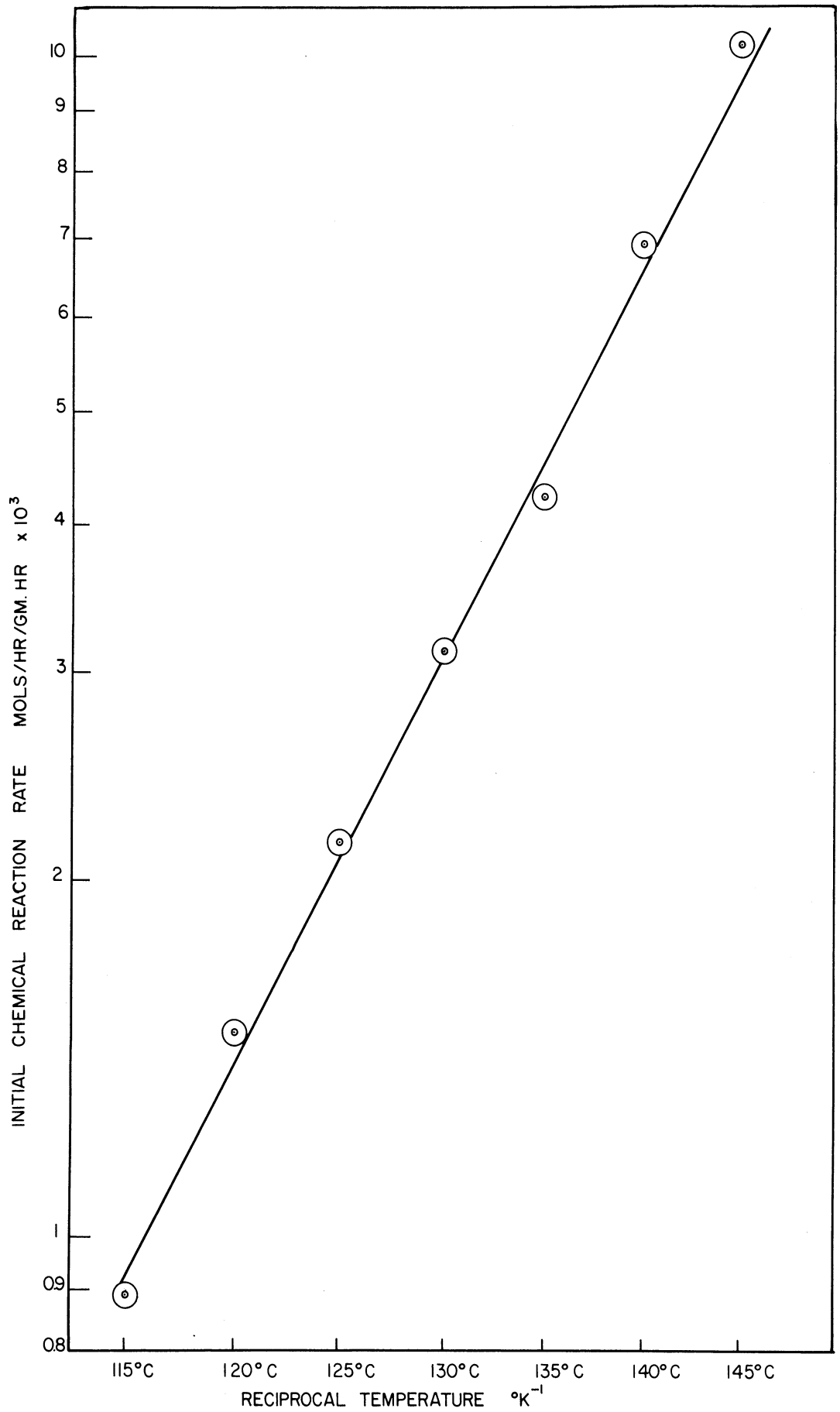

Figure 10. Effect of Temperature on Initial Reaction Rate.

represents a combination of constants of no theoretical significance, has a value of 9.0×10^{10}. The initial chemical reaction rate for the liquid phase hydration of butene-2 may be represented as:

$$r_i = 9.0 \times 10^{10} \exp(-24{,}800/RT) \quad \frac{\text{g mols}}{(\text{hr})(\text{gm HR})}$$

Since this rate equation is for a catalyzed reaction, the constants apply only for the particular catalyst used. For this purpose it is sufficient to describe the catalyst as a cation exchange resin of the sulfonated polystyrene type, crosslinked with 8% divinylbenzene.

Effect of Crosslinkage of Resin

The effective diffusivity of larger molecules in ion exchange resins has sometimes been found to decrease greatly with an increase in the percent crosslinkage of the polystyrene structure. This effect results from an increase in rigidity and a decrease in effective pore size as the divinylbenzene content is increased. In some cases it is possible to achieve very specific selectivity due to this effect. Although the study of the crosslinkage variable was not a major part of this research, results are available from one run (#49) in which 12% crosslinked resin was used rather than the 8% resin used throughout the rest of the investigation. A comparison of the reaction rate for this run with the rate for the same

temperature and space velocity (Figure 9), shows that the 12% crosslinked resin is only about 1/6 as efficient as the 8% resin. This large difference in effectiveness of the resins is not surprising considering the results obtained by some other investigators. It did however, indicate the desirability of using the customary 8% cross-linked resin for all subsequent runs.

Integral Reaction Rates with a Ternary Feed

Early in the experimental program four runs (25 - 28) were made using a ternary feed of the following composition:

A: 25 mol %

W: 15 mol %

B: 60 mol %

Figure 2 shows that at the temperature of the reaction this feed probably formed a single liquid phase in contrast to most of the later feeds which were within the two liquid phase envelope. At an intermediate space velocity, runs were made at four temperatures, 110°, 120°, 130° and 140°C. The conversion rates for these runs, illustrated by the arrows on Figure 11 indicate that some hydration occurred at 110°C, less hydration at 120°C, while by 130°C the reaction was proceeding in the opposite direction. The extent of dehydration was greatest at 140°C, but was apparently limited by a closer approach to equilibrium. These runs confirmed the effectiveness of the

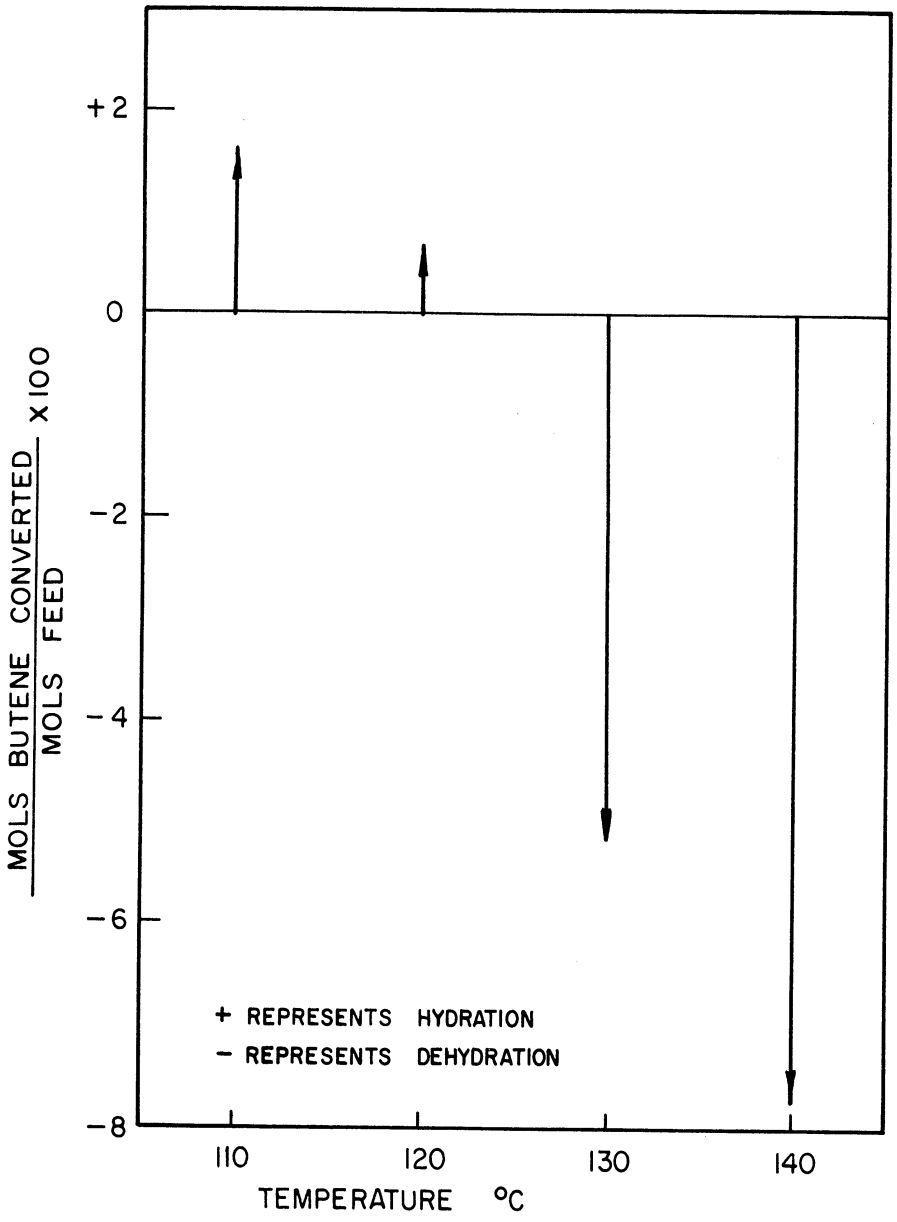

Figure 11. Effect of Temperature on Conversion for a Ternary Feed.

cation exchange resin as a catalyst for the reverse dehydration reaction. The results also indicate that, for the temperature range required for sufficient catalyst activity, the equilibrium alcohol concentrations would be fairly low. Since this study does not include the correlation of reaction rates for ternary liquid compositions, no further rate experiments were made with a three component feed.

Chemical Equilibrium

Because the measurement of chemical equilibrium implies the simultaneous occurrence of phase equilibrium, the discussion of these experiments is best considered with reference to a phase equilibrium diagram such as Figure 2, p 7. For a liquid phase reaction, the condition of chemical equilibrium may be represented by a thermodynamic equilibrium constant,

$$K_a = K_a\ (a_A,\ a_W,\ a_B),$$

which is dependent only on temperature. The same equilibrium data may be expressed as an equilibrium constant in terms of concentrations or mol fractions, as

$$K_x = K_x\ (x_A,\ x_W,\ x_B),$$

which is not only a function of temperature, but is a function

of two composition variables as well.

The K_x isotherms, representing compositions in chemical equilibrium, follow either of two forms when plotted on a ternary diagram. At sufficiently high values of K_x, the isotherm lies entirely in the single liquid phase region and is similar in shape to the liquid-liquid solubility curve (see Figure 2, p. 7). At lower values of K_x, which for the hydration reaction correspond to higher temperatures than in the first case, the chemical equilibrium isotherms intersect the phase equilibrium solubility curve (Figure 2). For the latter case, therefore, a chemical equilibrium composition isotherm follows a line from the pure butene corner until it intersects the solubility curve. The chemical equilibrium isotherm then becomes coincident with a phase equilibrium tie-line for the same temperature. From the intersection of this tie-line with the aqueous liquid phase, the isotherm changes direction sharply towards the pure water corner of the diagram. For the entire temperature range of interest in this investigation, the chemical equilibrium isotherms intersect the liquid-liquid solubility curve.

The selection of conditions which give a satisfactory approach to chemical equilibrium may be described most conveniently by reference to Figure 12. The series of arrows beginning at 0% alcohol represent the level of conversions obtained for a number of runs at low space velocity and with no alcohol in the feed (runs 64 - 69). It will be noted that

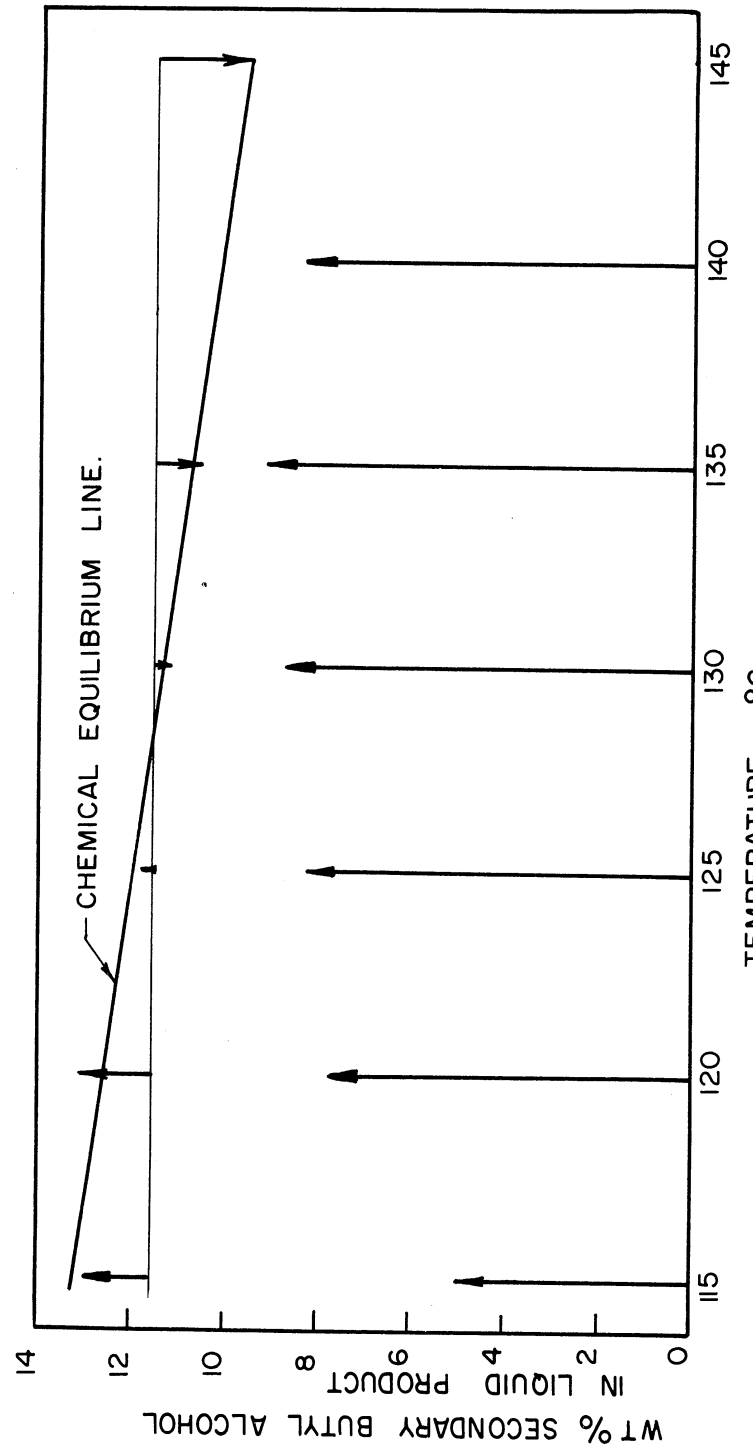

Figure 12. Effect of Temperature on Liquid Product Composition.

the extent of conversion, indicated by the length of the arrows, at first increases sharply with temperature, then levels off, and finally decreases with the last increase in temperature. This behavior indicates that at the higher temperatures the reactor product is closely approaching the limit of chemical equilibrium. From this series of runs an estimate of the equilibrium conversion curve was made, and an aqueous alcohol feed was prepared which would correspond to slightly less than the equilibrium conversion for the lower temperatures, and to slightly greater than the equilibrium conversion for the higher temperatures. The alcohol concentration in the liquid product corresponding to this feed is shown in Figure 12 as a horizontal base line, since it represents the condition of neither hydration nor dehydration occurring in the reactor. The series of arrows proceeding in either direction from this line represent the extent of reaction at various temperature levels, obtained when operating at the same low space velocity as for the first series of runs without alcohol in the feed. It may be noted that the choice of alcohol concentration in the feed was ideal, since at 115°, 120°, and 125°C, a very small amount of hydration occurred, while for higher temperatures the alcohol dehydrated to a slight extent. The conditions of these runs can therefore be considered as giving a satisfactory approach to equilibrium, so that equilibrium conversions can be calculated directly from the results.

The ternary feed used for the above series of runs is stoichiometrically equivalent to a butene-water binary feed

containing 76 mol % water. The results of both series of equilibrium runs are given in Table VIII, and are plotted on Figure 13. The smoothed data from Figure 13 have been cross-plotted on Figure 14 to show the effect of stoichiometric feed composition on equilibrium conversion, with temperature as a parameter. The particular value of representing the equilibrium conversions as shown on Figure 14 is that, within the two liquid phase region, interpolation between the high and low butene/water ratio data on this plot is by straight lines. The straight line interpolation follows readily from the fact that each pair of equilibrium conversion points must by definition fall on a phase equilibrium tie-line, which, in the units of this figure, is also a straight line. The use of mol ratios rather than mol fractions for the ordinate is equivalent to opening up the conventional closed triangle representation so that the apex of the latter (representing 100% alcohol) now lies at an infinite distance up from the butene-water base.

The equilibrium percent conversion of butene may now be conveniently calculated, and is shown on Figure 15, again as a function of stoichiometric feed composition and temperature. For purpose of comparison the equilibrium percent butene conversion for the high temperature, high pressure, vapor phase process has been reproduced on the same figure from Dale (7). The vapor phase data shown are for 385°C and various pressures from 1000 to 9000 psi. It is significant that the equilibrium conversions for the low temperature liquid phase process are

TABLE VIII

EXPERIMENTAL RESULTS FOR DETERMINATION OF CHEMICAL EQUILIBRIUM

Run	Resin[1]	Temp. °C	Feed Rate A gm/min	Feed Rate W gm/min	Feed Rate B gm/min	Equiv. Binary Feed mol % W	Space Velocity $^{-1}$ gms/mol/hr	Liquid Product Composition, wt % A/AW Duplicate Runs			Average	Stoichiometric Reactor Product A mol %	Stoichiometric Reactor Product W mol %	Stoichiometric Reactor Product B mol %	Mols Convd.[2] Mol Feed x 100	Integral Reaction Rate mols/hr/gm H R x 10^3
42,a	M	120	0.365	0.111	2.82	16.75	14.25	77.93			77.93	8.25	9.9	81.85	7.59	+ 0.13
45,a		135	0.367	0.111	2.82	16.76	14.25	77.92	77.60		77.76	7.8	10.4	81.8	7.16	- 0.18
46,a		140	0.366	0.111	2.83	16.69	14.25	77.92	78.59		78.24	7.8	10.35	81.85	7.17	- 0.20
47,a		130	0.358	0.109	2.83	16.43	14.25	78.75	78.98		78.87	7.9	9.8	82.3	7.29	+ 0.01
70,70b	P	115	0.065	0.449	0.401	76.25	26.2	12.91		13.00	12.97	3.02	75.6	21.4	2.95	+ 0.13
71,a,b		120	0.061	0.423	0.380	76.12	27.7	12.60	13.50	13.17	13.09	3.03	75.4	21.6	2.94	+ 0.13
72,a,b		125	0.061	0.423	0.394	75.58	27.4	12.51	11.28	11.20	11.66	2.70	74.9	22.4	2.60	+ 0.06
73,a,b		130	0.066	0.453	0.406	76.20	25.9	11.77	10.76	11.12	11.22	2.61	75.6	21.8	2.55	- 0.07
74,a,b		135	0.069	0.474	0.409	76.83	24.9	10.54	10.61	10.33	10.49	2.44	76.3	21.3	2.45	- 0.10
76,a,b		145	0.066	0.456	0.396	76.68	25.9		9.61	9.93	9.77	2.26	76.2	21.6	2.27	- 0.16

(1) See Table I for resin specifications

(2) Based on equivalent binary feed

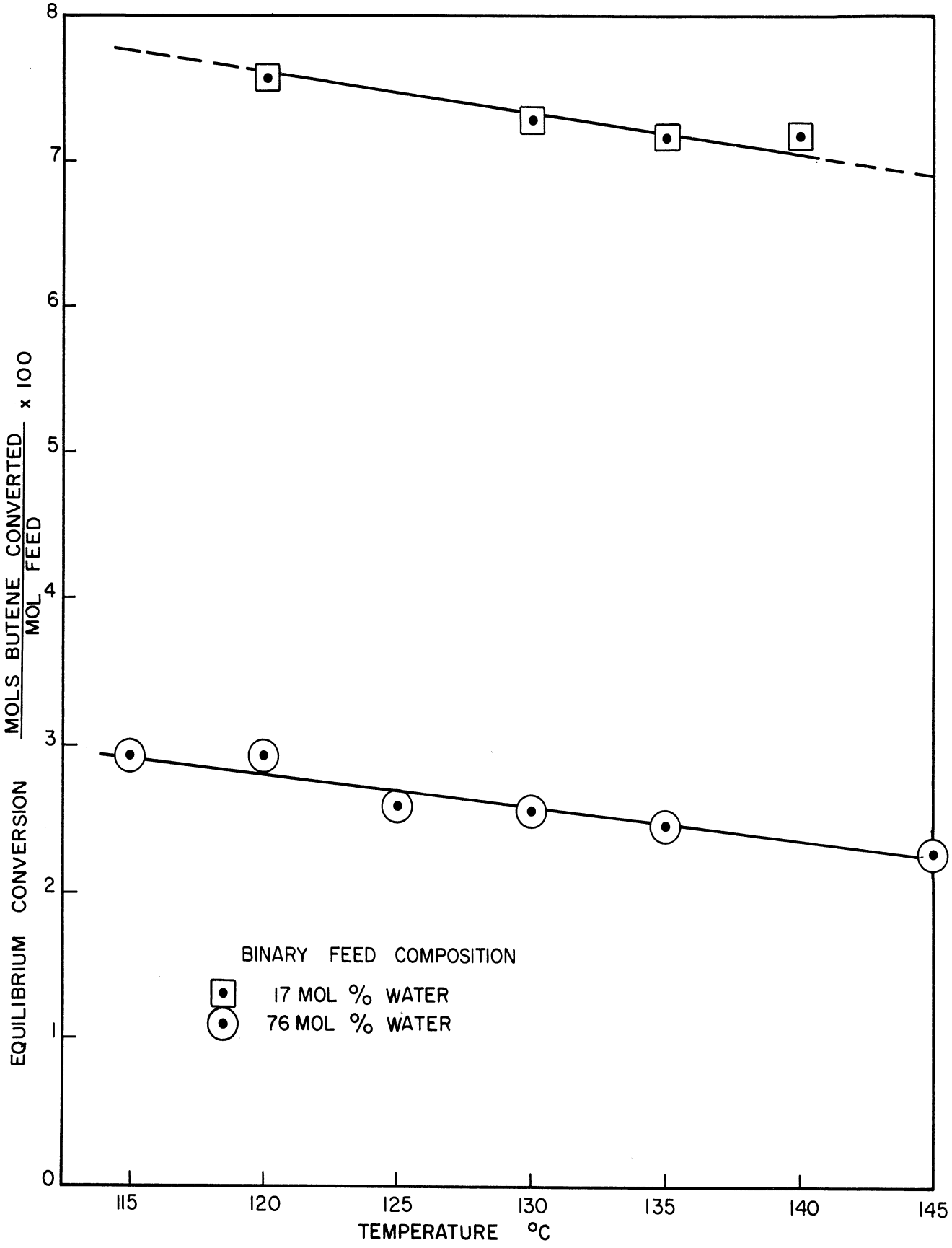

Figure 13. Effect of Temperature on Equilibrium Conversion for Two Binary Feeds.

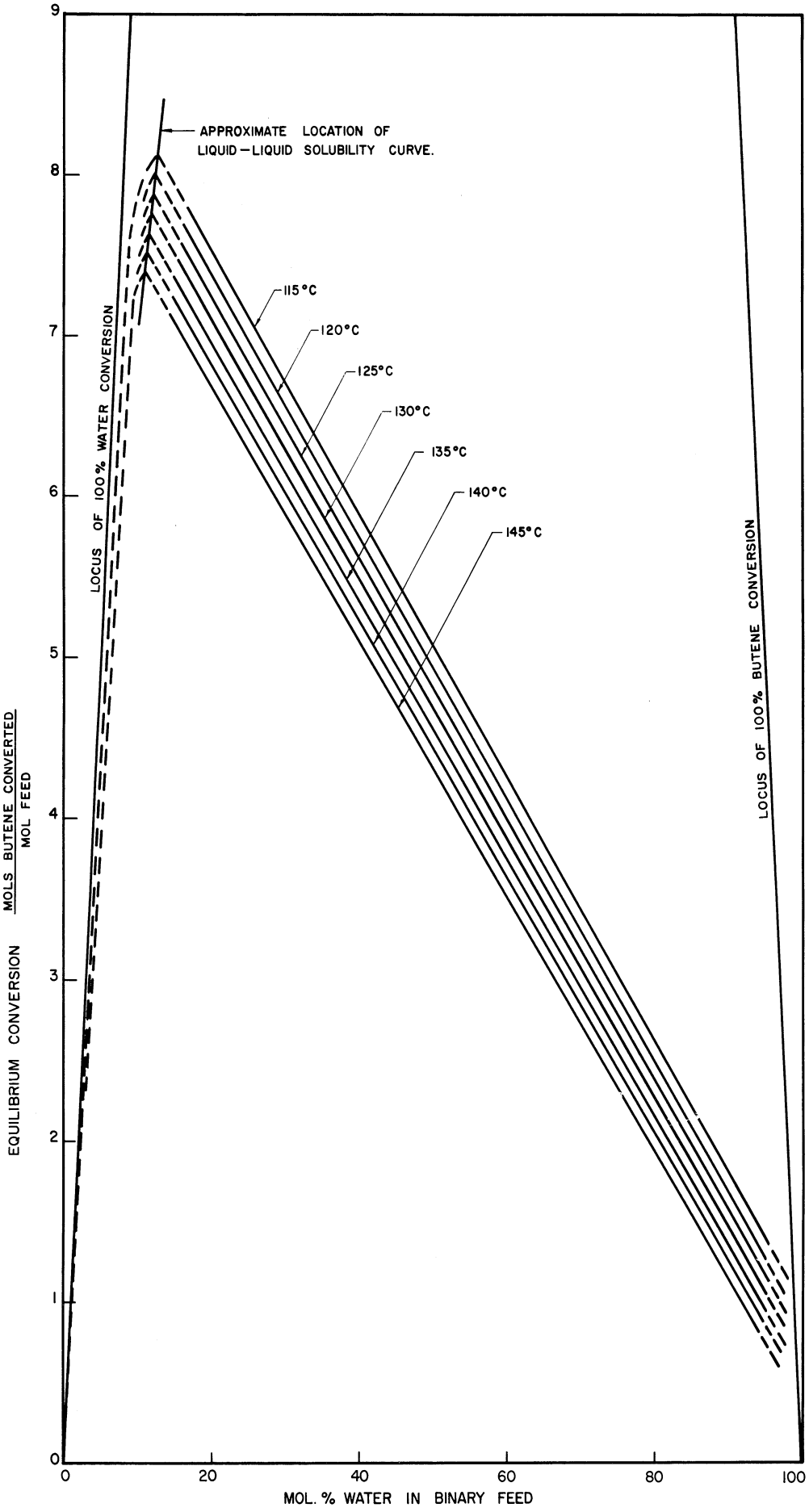

Figure 14. Effect of Feed Composition and Temperature on Equilibrium Conversion.

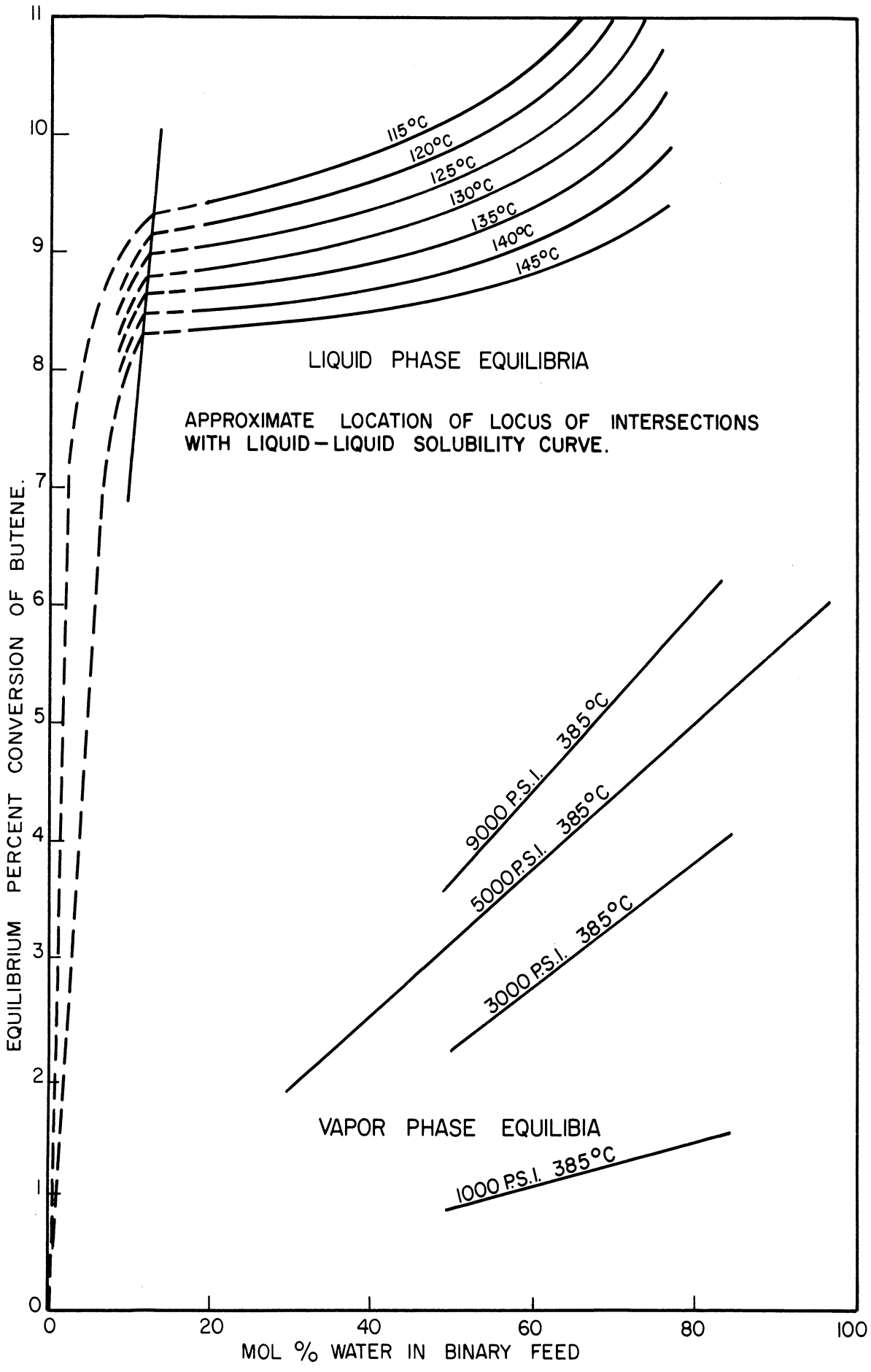

Figure 15. Equilibrium Conversion of Butene.

about two to four times the corresponding values for the high temperature, high pressure, vapor phase process.

As has already been indicated, the two sets of chemical equilibrium runs also give the slopes of a series of phase equilibrium tie-lines. The data of Figure 14 have been recalculated, therefore, in terms of mol percent, and are plotted on the phase diagram, Figure 16. The steep slope of these tie-lines substantiates the prediction made in the theoretical section that, except at very low alcohol concentrations, the alcohol content of the butene-rich phase would be much greater than that for the corresponding equilibrium water-rich phase.

It should be recalled that conventional chemical equilibrium constants cannot be calculated from this equilibrium data since the total compositions lie entirely within the two-phase envelope and neither of the actual phase compositions is known. While the calculation of equilibrium constants would have been desirable from a theoretical viewpoint, this lack is compensated by the practical utility of the equilibrium conversion plots.

Catalyst Life

Early runs were made with a thin Teflon film inserted in the reactor to prevent actual contact between the resin and the stainless steel reactor walls and thermowell. Since this

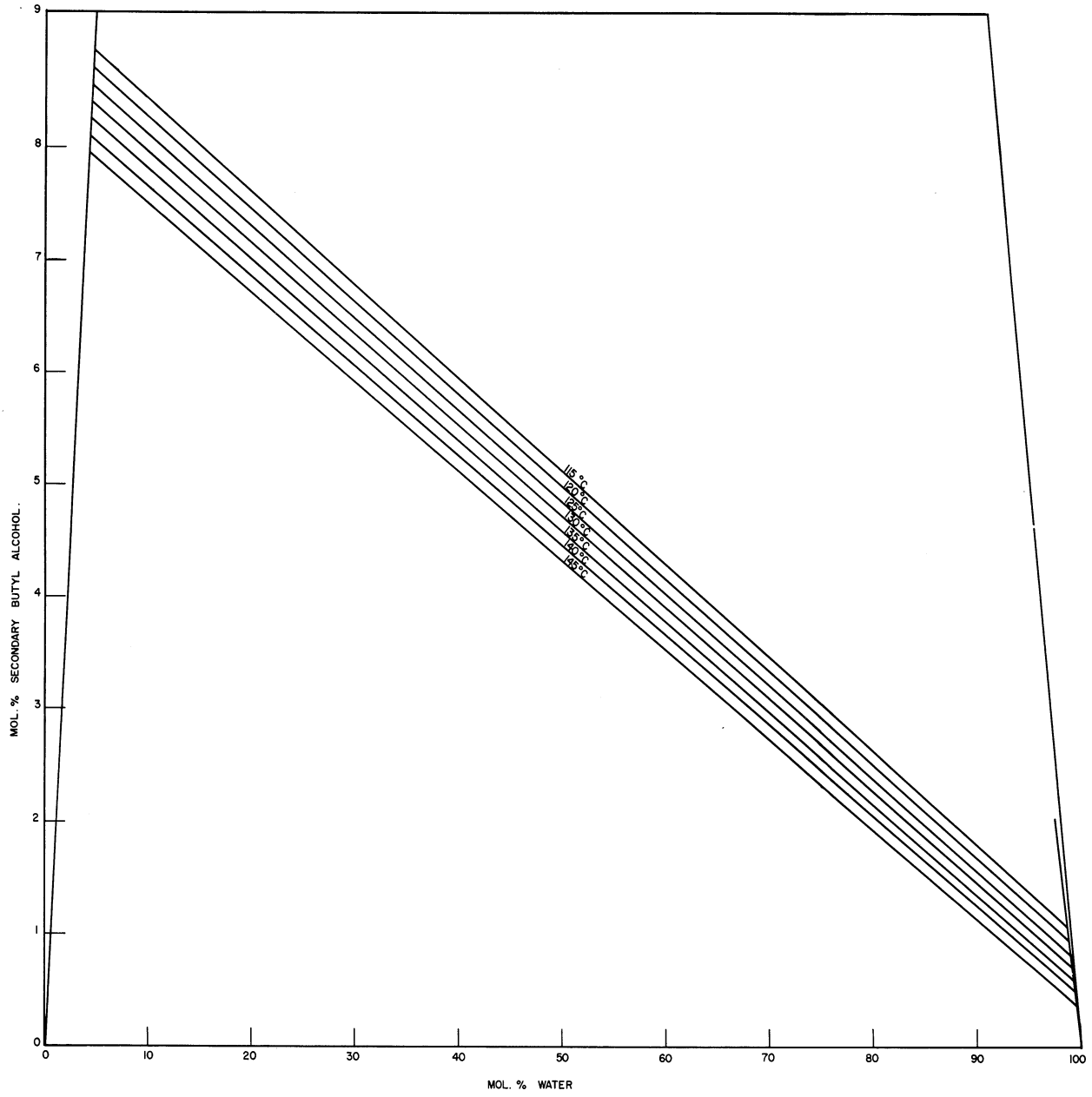

Figure 16 Isotherms Within Two-phase Region for Simultaneous Chemical and Phase Equilibrium

was not a bonded film, however, the steel surface was not completely isolated. Also, there were probably always some breaks in the Teflon barrier, allowing some direct contact between the resin and the steel walls. It was found that the resin darkened and lost acidity due to ion exchange after being used for some time in this environment. Also, rough estimates of the amount of metal sulfates and free sulfuric acid in the liquid product indicated a very high rate of resin desulfonation. Results from two of these runs are listed below:

Temperature °C	Desulfonation rate % per day	Time to 50% desulfonation days
130°	2.0	25
140°	11.5	4.4

Subsequently the reactor walls and the thermowell were sealed off by tightly fitting tantalum liners, as described earlier. Since the sulfuric acid, liberated by resin hydrolysis, was no longer converted partially to the metal sulfates, the desulfonation rate could be measured simply by the rate of sulfuric acid production. The sulfuric acid concentration of the liquid product was measured by a Beckman pH meter, calibrated with standard buffer solutions. The data pertaining to resin desulfonation rates are presented in Table IX. The resin life, expressed as the time required for 50% hydrolysis of the resin, and calculated using the initial resin hydrolysis rate, is plotted on Figure 17. The lines on

Table IX

Run	Temp °C	Resin charge equivs.	Liquid product ccm.	pH	Time to 50% hydrolysis, yrs.
59a	125	0.264	2.03	5.3	24
60b	130		2.03	5.4	30
61,a,b	135		2.11	5.1	17
62,a	140		2.12	4.9	9
63	145	0.264	1.90	4.3	27
64,a	115	0.263	0.53	4.4	11
65	120		0.57	4.5	15
66	125		0.63	4.4	20
67,a	130		0.61	4.3	10
68,a	135		0.59	4.05	4.7
69,a	140	0.263	0.62	3.8	2.8
87	115	0.0843	4.42	6.4	46
88	120		4.59	6.35	41
89	125		4.5	6.2	30
90	130	0.0843	4.37	6.15	27
98	135	0.025	4.12	6.25	10
99	140		4.43	6.3	11
100	145	0.025	4.53	6.45	15

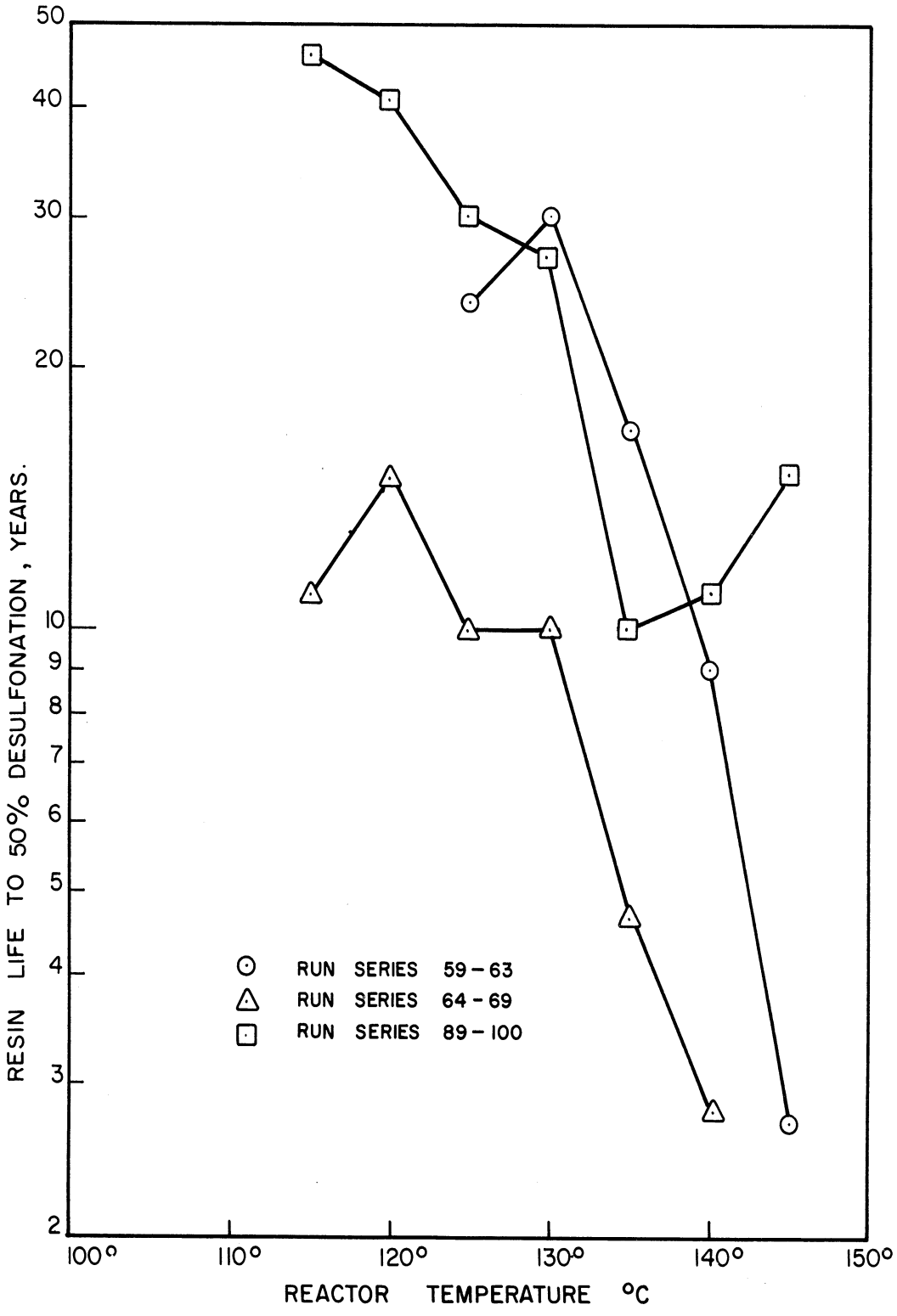

Figure 17. Effect of Temperature on Resin Life.

this plot serve only to connect points of the same series of runs. From the hydrolysis rates obtained, it is apparent that resin stability is not an important factor in its use as a catalyst for this reaction over the range of temperatures investigated.

In addition to loss of catalytic activity by desulfonation, some authors have noted a fouling of the ion exchange resin by reaction products or by-products. For example, Klein and Banchero (15), using the same resin as in the present study, noted that the resin turned completely black within a very short time when it was used as a catalyst for acetone condensation. They concluded that the black color resulted from the deposit of a tarry product of the reaction. In the present study the resin at first turned dark during use, as already noted, but this was due only to ion exchange with the steel walls of the reactor at high temperatures. Once the resin had been protected from ion exchange with the walls, it became impossible to visually distinguish used resin from the fresh material.

Hydration of Propylene to Isopropyl Alcohol

In order to establish the effectiveness of the cation exchange resin as a catalyst for monoolefins other than normal butene, a few exploratory runs were made using propylene. The operating conditions are summarized in Table X. A gas and liquid product were collected in equilibrium at 25°C and 1 atm.

Table X

Summary of Propylene Hydration Runs

Run	T °C	P psi	F_v c.c.m. inlet	P/W in feed mol ratio	P/W in feed mol ratio	Reaction Rate mols IPA / (hr)(gm HR)	% Conversion P	% Conversion W	Wt. % IPA lqd. prod.	F/W mols/hr / gm HR
81	145°	1000	13.4	1.3/1	19/1	0.0100	21.1	27.9	53.6	0.0526
81a	145°	1000	14.2	0.88/1	12.7/1	0.0117	23.9	21.1	44.6	0.0607
82	145°	2500	3.1	0.44/1	2.5/1	0.0051	24.7	10.6	26.7	0.0346
83	145°	500	33.5	0.80/1	30/1	0.0054	13.1	10.6	23.8	0.0530
84	135°	500	34.1	0.67/1	27.5/1	0.0046	10.6	7.1	16.0	0.0586

8% XL Dowex 50

as before. The isopropanol content of the liquid was analyzed by density, with a small correction required for the effect of dissolved propylene. No allowance was made for the small amount of isopropyl ether believed to have been present. The small alcohol and water content of the equilibrium flash gas was estimated from vapor pressure data and vapor-liquid for the isopropanol-water system. Since it was not planned to subject the results of the few propylene hydration runs to any kinetic analysis, the runs were carried out rapidly with the operating conditions less carefully controlled than for the butene runs. The results are summarized in Table X.

At reactor inlet conditions, the propylene-water feed will form two phases as in the case of butene-water feeds. Since in this case, however, the temperatures used are all above the critical temperature of propylene (T_c = 91.4°C, P_c = 668 psia), the propylene-rich phase may not properly be called a liquid phase, but rather a dense fluid phase. Although the highest conversion of propylene obtained is not sufficient to yield a single liquid (or fluid) phase at any point in the resin bed, the mutual solubilities of the two fluid phases, (i.e. the water concentration in the olefin-rich phase and the olefin concentration of the water-rich phase) are much greater than for the butyl alcohol system.

A comparison of the reaction rates and conversions obtained in the propylene hydration runs with those already discussed for butene hydration, shows that both the resin catalyzed reaction rates

and the chemical equilibrium are much more favorable for the propylene system. The high catalytic efficiency of the cation exchange resin for another olefin hydration is particularly interesting.

Estimates of resin life based on desulfonation rates during the propylene hydration runs indicated a surprisingly rapid desulfonation of the resin. Since steady state conditions were only roughly approximated for these runs, the estimates of desulfonation rates are quite erratic. However, the average rate for the four runs at 145°C indicated 50% hydrolysis in 60 days, while the single run at 135°C indicated 50% hydrolysis in 110 days. While the resin hydrolysis rates appear moderately high, it should be noted that on the basis of isopropyl alcohol production, these rates correspond to only 0.0006 pounds resin desulfonated per pound isopropyl alcohol produced at 135°C, and 0.0007 pounds resin per pound alcohol at 145°C. On the basis of alcohol produced, therefore, the catalyst consumption is still very low.

Butene Hydration by Two Step Process (Esterification-Hydrolysis)

The two-step process of producing secondary butyl alcohol is favored industrially over those continuous catalytic processes which have been investigated prior to this time. In the two-step process, the butylene is first esterified with the sulfuric acid to form the mono-butyl sulfate, which is hydrolyzed in the second step to the secondary alcohol. The

reactions may be represented as:

Esterification: $C_4H_8 + H_2SO_4 = C_4H_9 \cdot HSO_4$

Hydrolysis: $C_4H_9 \cdot HSO_4 + H_2O = C_4H_9OH + H_2SO_4$

Many other reactions are likewise carried out using an inorganic acid, not as an orthodox catalyst, but to produce a chemical intermediate which is treated further to obtain the desired product. Although a cation exchange resin may in many respects be considered as a solid strong acid, no comparable use of the resin has yet been noted in the literature. Thus it was considered of considerable theoretical as well as practical use to determine whether the cation exchange resin could function in a manner analogous to sulfuric acid in the two step hydration process.

The runs were carried out in a stainless steel reactor before it was recognized that the steel surfaces had to be completely isolated from the resin bed. As a result, most of the hydrogen ions in the fresh resin had been exchanged for metal ions from the steel surfaces by the time the runs were completed and the resin removed. For this reason the results are not presented as more than semi-quantitative.

The sequence of operations for these runs may be summarized as follows:

(1) Water and alcohol from the hydrolysis step is flushed from the void volume of the resin bed with butene.

(2) When the flushing is complete, the void volume of the bed is left filled with liquid butene at the temperature and pressure desired for the esterification step.

(3) At the end of the esterification time an amount of butene equivalent to the void volume of the bed is withdrawn and is replaced with the desired amount of water for hydrolysis of butyl sulfonate resin ester.

(4) For complete hydrolysis of the resin, the aqueous alcohol solution may be displaced with additional aliquots of hydrolysis water. The cycle of operations is completed by displacement of the final aqueous solution of the hydrolysis step in the manner described in (1).

The range of variables studied includes:

Esterification	time	0.5 - 13 hours
	temperature	55° - 135°C
	pressure	500 - 10,000 psi.
Hydrolysis	time	0.25 - 20 hours
	temperature	55° - 135°C
	pressure	100 - 9500 psi.

In addition to the gradual loss of catalyst activity due to exchange of hydrogen ions for metal ions, another major source of uncertainty results from the carry-over of alcohol from one run to the next, particularly for the earlier runs

when insufficient hydrolysis water was used.

The calculation of percent conversion of n-butene is based on the amount of butene contained in the void volume of the bed. The corresponding percent esterification of the resin is based on the equivalents of acidity originally present, although the true percent esterification for the later runs must be greater than the calculated values due to loss of resin acidity. The results of all the esterification-hydrolysis runs are summarized in Table **XI.**

No quantitative relations can be derived from this data due to the sources of error already described. In general, the increase of both extent of esterification and of hydrolysis with time and with temperature can be seen. As might be expected, the esterification of water saturated resin appears to be much slower than the subsequent hydrolysis. The importance of pressure on esterification rate is less clear. The most significant result is, of course, that the process works at all with cation exchange resin substituted for sulfuric acid. The butyl alcohol production rates by this method are, however, lower by a factor of about three as compared to the continuous catalytic hydration process. The postulated reactions may be represented as:

Esterification: $C_4 H_8 + \phi SO_3^- H^+ = \phi SO_3 \cdot C_4 H_9$

Hydrolysis: $\phi SO_3 \cdot C_4 H_9 + H_2O = C_4 H_9 OH + \phi SO_3^- H^+$

TABLE XI

EXPERIMENTAL RESULTS FOR TWO-STEP ESTERIFICATION-HYDROLYSIS PROCESS(1)

Run	Esterification Conditions Time hrs	mins	Temp. °C	Pressure psi	Hydrolysis Conditions Time hrs	mins	Temp. °C	Pressure psi	Hydrolysis Water, ml	Liquid Product ml	wt % A	Alcohol Produced gms	gm total	% Conversion of H R	Butene
1	2		54	9500		50	58	200	16	20	0.6	0.12	0.12	0.4	0.3
2	5	20	62	9500		15	66	9000	60	7	0.6	0.04			
					13	20	71	1000		52	0.7	0.36	0.40	1.3	1.0
3	3	20	80	10,000	8	40	84	400	50	22	0.6	0.13			
										30	0.5	0.15	0.28	0.9	0.7
4	10	30	80	8000	4	30	88	400	41	40	1.5	0.6	0.6	2.0	1.6
5	7		116	5000	13		121	700	45	19	2.3	0.4			
										26	4.5	1.2			
										25	1.8	0.5	2.1	6.9	5.5
6	6		95	8000	11	45	100	nil	45	18	1.8	0.3			
										15	1.9	0.3	0.6	2.0	1.6
7	4		107	5000	11	15	110	nil	40	3	4.8	0.14			
										17	1.4	0.24	0.38	1.3	1.0
8	9	20	110	1900	5	40	110	nil	40	6	11.5	1.0			
										23	3.0	0.7	1.7	5.6	4.5
9	5	30	112	8000	11		112	nil	35	27	9.3	2.5	2.5	8.1	6.5
10	5	40	112	600	6	25	112	nil	36	32	4.3	1.4	1.4	4.5	3.6
11		28	110	9800		35	110	nil	35	30	1.2	0.33	0.33	1.2	0.9
12	12	45	110	1600	11	40	110	nil	73	27	8.9	2.4			
										33	3.1	1.0	3.4	11.0	8.8
13		41	116	8000	37	35	110	nil	35	34		0.43	0.43	1.4	1.1
14		46	110	9500	6	10	110	nil	72	41	1.4	0.56			
										32	1.6	0.51	1.07	3.6	2.9
15	10	20	110	650		39	109	nil	70	37	5.9	2.2			
										40	1.5	0.6	2.8	9.1	7.3
16	1	27	108	9500		34	108	7000	70	37	0.7	0.26			
										27	0.3	0.37	0.63	2.0	1.6
17	1	48	108	700		24	108	600	72	37	0.9	0.33			
										29	2.8	0.81	1.1	3.6	2.9
18	2	20	108	3400		12	110	3000	70	38	1.1	0.42			
										28	1.6	0.45	0.87	2.9	2.3
19	6	20	119	600		24	119	700	70	38	4.3	1.6			
										30	4.6	1.4	3.0	11.7	7.8
20	9	15	119	8000	3	50	119	3000	134	37	8.4	3.1			
										37	3.2	1.2			
										27	3.2	0.9			
										37	1.6	0.6	5.8	18.9	15.1
21		37	121	9500		48	119	5000	134	37	1.1	0.41			
										24	1.6	0.38			
										20	1.5	0.30			
										83	0.5	0.42	1.5	4.9	3.9
22	1	20	121	9700	1	55	125	2000	121	46	2.5	1.2			
										27	0.6	0.2			
										18	0.9	0.3	1.7	5.4	4.4
23	2	45	135	9700	1	55	135	500	85	48	4.0	1.9			
										36	3.9	1.4			
										40	0.3	0.1			
										64	nil	nil	3.4	11.0	8.8

(1) Catalyst Charge: 82.3 gms, 8% DVB
Dowex 50 resin

While these reactions represent the stoichiometry of the overall reaction, the present exploratory investigation is not sufficient to define the reaction mechanism involved.

VII CONCLUSIONS

1. A sulfonated polystyrene type ion exchange resin is an active catalyst for the hydration of n-butene to sec.-butyl alcohol and for the reverse, or dehydration reaction.

2. The presence of two liquid phases which are almost completely immiscible causes a large reduction in reaction rate due to liquid phase mass transfer resistance except when flow conditions corresponding to a high Reynolds modulus are used.

3. Resin phase diffusional resistance is not a major problem in this system; 100 - 200 mesh size gives a resin of 97.3% volumetric efficiency.

4. Equilibrium butene conversions for the liquid phase hydration process are higher by a factor of two to four than those for the high temperature, high pressure vapor phase process.

5. The slope of phase equilibrium tie-lines in the two liquid phase envelope may be determined by measuring chemical equilibrium conversions for a high and a low butene/water feed.

6. The life of the resin catalyst in the butene hydration environment is sufficiently long that this factor is not an important consideration determining its use.

7. The effectiveness of the cation exchange resin as a hydration catalyst extends to propylene, the next mono-olefin in the homologous series.

8. The cation exchange resin will replace the functions of sulfuric acid in the two-step esterification-hydrolysis process. This is partial evidence that the sulfonated resin can enter into chemical reactions to form solid intermediate reaction products. The results available from this series of experiments are not sufficient, however, to provide a definite answer to this question.

APPENDIX A

Differential Vacuum Distillation Calculations

In order to calculate the change in alcohol/water ratio which results from the differential distillation to remove butene, a conventional Rayleigh distillation calculation is carried out. A sample calculation for one set of conditions will be shown, followed by a graphical summary of the distillation corrections.

For this system, the requirement of vapor-liquid equilibrium throughout the distillation may be represented as

$$\frac{dn_{AW}}{dn_B} = \frac{p_{AW}}{p_B} \qquad (1)$$

where n_{AW}, n_B = mols alcohol and water, and mols butene in the liquid. If an 81.7 wt. % A/AW solution is selected for the sample calculation, then, from Figure 18, p_{AW} = 37mm. Also, from the data reported in Table II and Figure 8 on the solubility of butene in aqueous alcohol solutions, the following relation may be used to relate x_B to p_B:

$$x_B = \frac{\alpha\, p_B}{P^{\circ}_B} \qquad (2)$$

where x_B = mol fraction butene in the liquid

P°_B = vapor pressure of pure butene at 25°C

= 1800 mm mercury

α = non-ideality factor, a function of the alcohol/water ratio

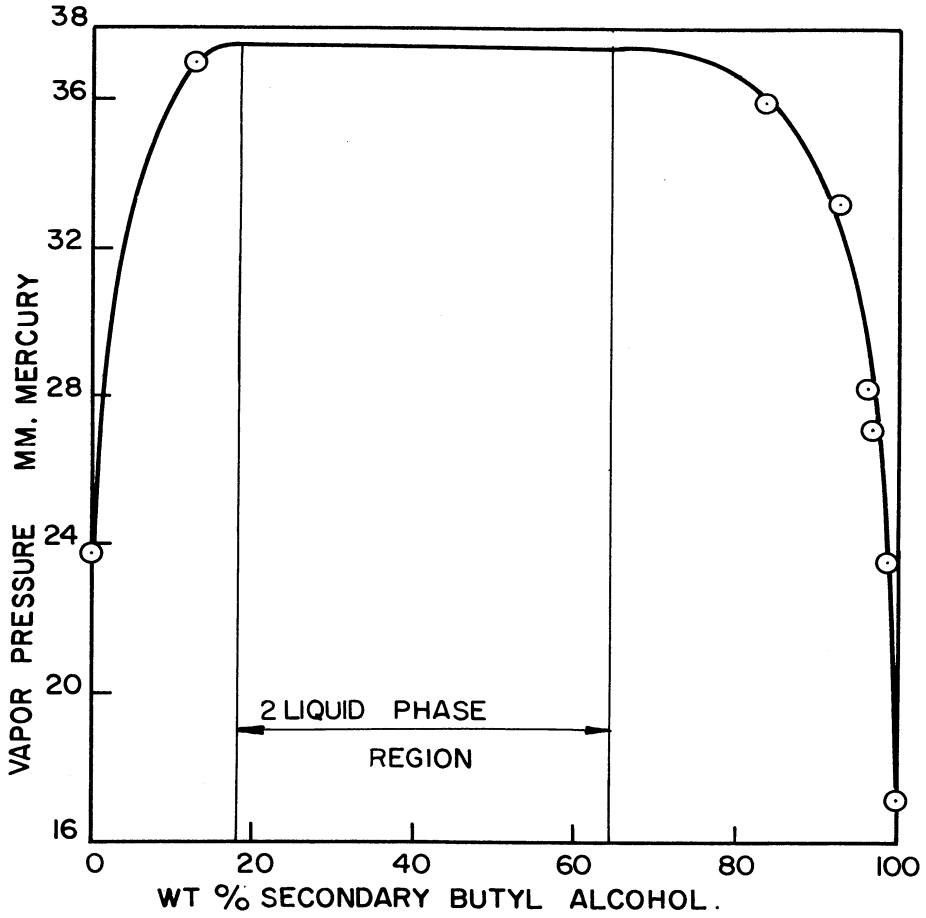

Figure 18. Vapor Pressure at 25°C for Secondary Butyl Alcohol-Water.

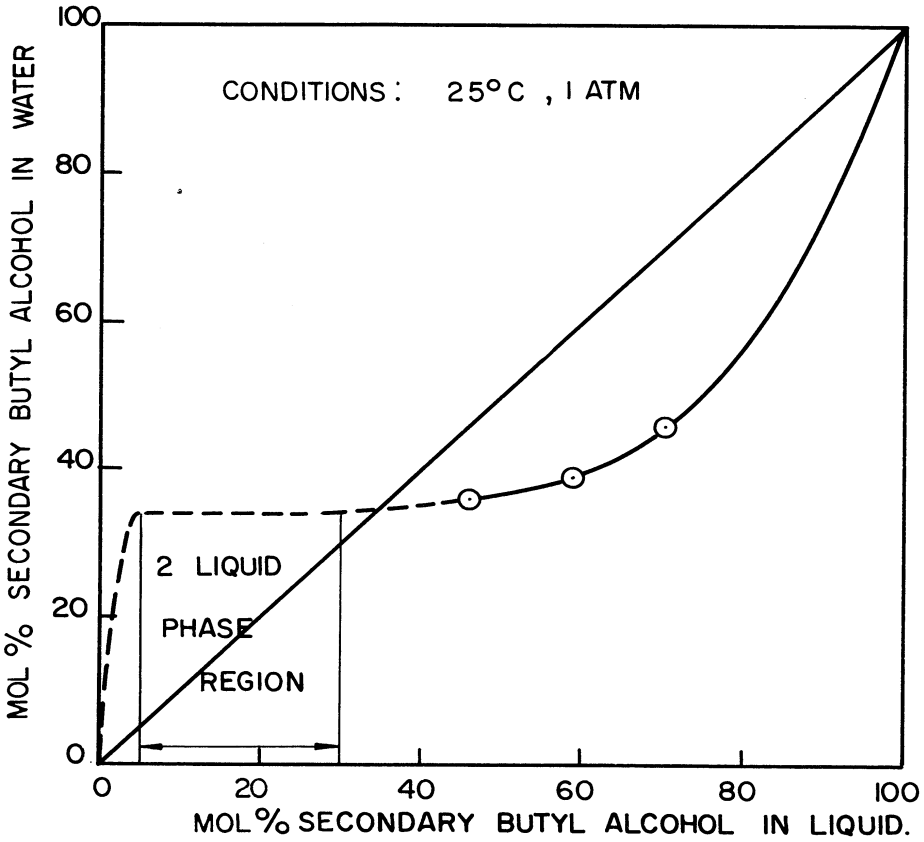

Figure 19. Vapor-Liquid Equilibrium for Secondary Butyl Alcohol-Water.

$$= 0.168 \text{ for } 81.7 \text{ wt \% A/AW}$$

The material balance equation

$$d\, n_B = (n_{AW} + n_B)\, d\, x_B \qquad (3)$$

may then be combined with equations (1) and (2) to give

$$dn_{AW} = \frac{\alpha\, p_{AW}\, (n_{AW} + n_B)_{ave}}{P^{\circ}_B} \quad \frac{dP}{P - p_{AW}} \qquad (4)$$

where P = the variable distillation pressure, mm mercury

$(n_{AW} + n_B)_{ave}$ = average total mols in liquid per mol of original butene saturated liquid. For the 81.7 wt. % A/AW solution, it will be seen that $(n_{AW} + n_B)_{ave} = 0.97$ is a satisfactory mean value. Equation (4) may then be integrated to calculate any final value of $(P - p_{AW})_f > 0$. The following integrated equation is obtained by substitution of the stated values of the constants:

$$\Delta n_{AW} = 7.1 \times 10^{-3} \log \frac{710}{(P - 37)_f} \qquad (5)$$

The calculation is completed for any value of final distillation pressure by assuming the relatively small amount of butene present does not affect the alcohol/water relative volatility. With this assumption, the binary vapor-liquid data of Figure 19 may be used to calculate Δn_A and Δn_W from the value of Δn_{AW} given by equation (5).

Since the final measurement after distillation is to be a density determination, the small effect on density of the butene not removed by the distillation must also be considered. Measurements of density of butene saturated alcohol solutions show that, in this range, 1 wt. % butene has the same effect on density as 1.3 wt. % butyl alcohol. It follows, therefore, that the distillation correction should pass through a minimum when determined as a function of final distillation pressure. If the final distillation pressure is not sufficiently low, the correction will be large due to the effect on density of the considerable amount of butene left in the final solution. Conversely, it may be seen from equation (5) that as the final pressure is reduced, $(P - 37)_f \rightarrow 0$, and Δn_{AW} becomes large due to the differential distillation effect, and the correction will again become large.

These calculations were completed for a number of alcohol/water ratios and for a number of different final pressures. Some of the results are summarized on Figure 20. From the optimum indicated by these figures, a final pressure $(P - p_{AW})_f$ = 7 mm was selected as a standard for all distillations run.

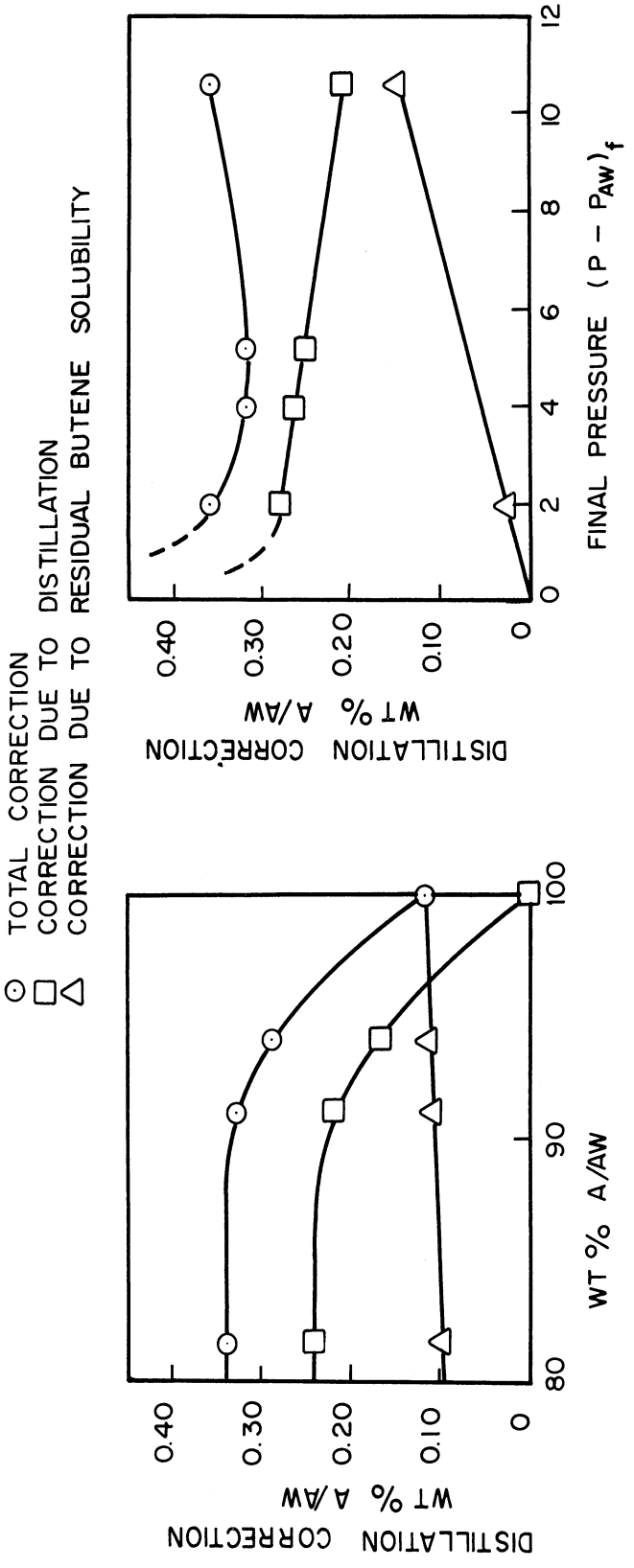

Figure 20. Differential Distillation Correction Factors.

APPENDIX B

Gas Product Analysis

No simple and accurate method of analysis was available for the secondary butyl alcohol and water content of the saturated vapor product. However, since the amount of alcohol and water leaving in the gas product was in general much less than in the liquid product, it was considered satisfactory to calculate the analysis from vapor pressure and vapor-liquid equilibrium data for the alcohol-water binary. The calculated compositions will be in error to the extent that the behavior of the vapor deviates from Dalton's law of ideality, and the alcohol-water relative volatility is affected by the small amount of butene dissolved in the liquid phase. Since most of the data are for dilute aqueous alcohol solutions, that is, below the liquid-liquid solubility limit (see Figure 8, p. 42), only the calculations for this range of products will be shown. The calculation for the more concentrated products is completely analogous to those illustrated.

Liquid product composition, x_A = 11.6 wt. % = 3.09 mol % A/AW

From vapor-liquid equilibrium data, Figure 19, p. 86, y_A = 28 mol% A/AW.

From vapor pressure data at 25°C, Figure 18, p. 86, p_{AW} = 36.7 mm for x_A = 11.6 wt. %

$$\therefore \quad y_A = \frac{p_A}{P} = \frac{y_A\, p_{AW}}{P} = \frac{(0.28)(36.7 \text{ mm})}{(744 \text{ mm})} = 1.39 \text{ mol \%}$$

$$\text{and} \quad y_W = \frac{p_W}{P} = \frac{y_W\, p_{AW}}{P} = \frac{(0.72)(36.7\ \text{mm})}{(744\ \text{mm})} = 3.55\ \text{mol \%}$$

$$\therefore \quad y_B = \frac{95.06}{100.00}\ \text{mol \%}$$

In this way a graph was prepared giving vapor composition as a function the alcohol content of the liquid product.

NOMENCLATURE

a	activity
A	sec-butyl alcohol; frequency factor in Arrhenius equation; cross-sectional area of reactor
AW	sec-butyl alcohol and water
B	n-butene
C	reactant concentration
C.S.T.	critical solution temperature
D.V.B.	divinylbenzene
E	energy of activation
F_m	molar flow rate
F_v	volumetric flow rate
HR	hydrogen form of cation exchange resin
k	reaction rate constant
K_a	equilibrium constant in terms of activities
K_x	equilibrium constant in terms of mol fractions
n	mols component in liquid
p	partial pressure
psi	pressure, pounds per square inch
P	pressure
P°	vapor pressure of pure component
r	reaction rate
R	resin radius; gas constant
Re'	modified Reynolds number
T	absolute temperature, ° Kelvin

W	water; weight of catalyst
x	mol fraction in liquid
y	mol fraction in vapor

Greek letters

α	phase distribution coefficient; non-ideality factor
	penetration function in resin efficiency function
Δ	increment
$\emptyset$	volumetric efficiency of the resin

Subscript

f	final
i	initial
I	integral
m	molar
p	particle
v	volumetric

BIBLIOGRAPHY

1. Annual Reviews of Physical Chemistry: Ion Exchange, 1951-1957, Annual Reviews Inc.

2. Annual Reviews of Unit Operations: Ion Exchange, Ind. Eng. Chem., 1948-1958.

3. Barker, G.E. and R.R. White, Chem. Eng. Prog. Symp. Series No. 4, 48, 75 (1952).

4. Bauman, W.C., J.R. Skidmore and R.H. Osmun, Ind. Eng. Chem. 40, 1350 (1948).

5. Boyd, G.E., B.A. Soldano, and O.D. Bonner, J. Phys. Chem. 58, 456 (1954).

6. Clough, W.W, and C.O. Johns, Ind. Eng. Chem., 15, 1030 (1923)

7. Dale, C.B. "Vapor Phase Hydration of Butene-2 to Butanol-2 at High Pressures" (Ph.D. Dissertation, University of Michigan, 1955.

8. Dale, C.B., C.M. Sleipcevich and R.R. White, Ind. Eng. Chem., 48, 913 (1956).

9. Denel, H., Mitt. Lebensm. Hyg. 46, 12 (1955).

10. Ellis, C., The Chemistry of Petroleum Derivatives, Vol. II, Chp. 11, Chem. Cat., 1937.

11. Goldstein, R.F. The Petrochemicals Industry, Chp. 7, Spon, 1949.

12. Gregor, H.P., K.M. Held, B.R. Sundheim, and M.H. Waxman, J. Coll. Sci. 7, 516 (1952)

13. Helfferich, F., J. Am. Chem. Soc. 76, 5567 (1954).

14. International Critical Tables, Vol. III, p. 388, McGraw-Hill Book Company, New York, 1928.

15. Klein, F.G. and J.T. Banchero. Ind. Eng. Chem., 48, 1278 (1956).

16. Kunin, R., Ion Exchange Resins, 2nd Ed. p. 259, J. Wiley & Sons, Inc., New York, 1958.

17. Lister, B.A.J., Ind. Chemist, 32, 257 (1956).

18. Marek, L.F., and R.K. Flege, Ind. Eng. Chem. 24, 1428 (1932).

19. Nachod, F.C. and J. Shubert, Ion Exchange Technology, Chp. 11, Academic Press, 1956.

20. Pepper, K.W., J. Appl. Chem. 1, 124 (1951).

21. Saletan, D.I. and R.R. White, Chem. Eng. Prog. Symp. Series No. 4, 48, 59 (1952).

22. Seidell, A. and W.F. Linke, Solubility of Inorganic and Organic Compounds, Supplement to the 3rd Edition, D. Van Nostrand Company, Inc., New York 1952.

23. Sleipcevich, C.M. "Design, Construction and Operation of a High Pressure High Temperature Plant" (Ph.D. Dissertation, University of Michigan, 1947).

24. Sleipcevich, C.M. and G.G. Brown, Chem. Eng. Prog. 46, 556 (1950).

25. Smith, N.L. and N.R. Amundsen, Ind. Eng. Chem. 43, 2156 (1951).

26. Stanley, H.M., J.K. Youell, and J.B. Dymock, J. Soc. Chem. Ind. 53, 204T, (1934).